

GROWTH AND STATUS OF THE ARGONNE PREMIUM COAL SAMPLE PROGRAM

Karl S. Vorres
Chemistry Division, Building 211
Argonne, IL 60439

Keywords: samples, premium, information

ABSTRACT:

The Argonne Premium Coal Sample Program (APCSP) was established to provide samples to the basic coal research scientific community. The quality of these samples is intended to be the best that can be devised and implemented. Samples of eight U. S. coals have been selected, collected, processed and packaged, analyzed and distributed. Information has been disseminated through Symposia, Quarterly Newsletters, and a Users Handbook. The number of publications is now about 1 for each two shipments of coal samples, and is approaching 200.

INTRODUCTION:

There has been a need for a set of coal samples that can be compared and provide a basis for meaningful correlations, and that will also be stable over long periods of time. This set of samples must also be available over a long period of time to permit as extensive a set of studies to be done with this set of samples as the research community would need.

In response to the need and with the support of the U. S. Department of Energy, Office of Basic Energy Sciences, Chemical Sciences Division, the Argonne Premium Coal Sample Program (APCSP) was initiated. A set of eight U. S. coals was selected to represent a range of chemical parameters of importance (carbon, hydrogen, sulfur and oxygen content) as well as maceral concentrations, and paleobotanic origins. These coals were carefully collected with the help of personnel from the U. S. Geological Survey and the Pittsburgh Testing Laboratory.

The eight coals are indicated in Table I, below.

Table I. Argonne Premium Coal Samples and Some Characteristics

#	Seam	State	Rank	C	H	O	S	Ash
1	Upper Freeport	PA	Med. Vol. Bit.	86	4.7	8	2.3	13
2	Wyodak-Anderson	WY	Subbituminous	75	5.4	18	0.6	9
3	Illinois #6	IL	High Vol. Bit.	78	5.0	14	4.8	15
4	Pittsburgh (#8)	PA	High Vol. Bit.	83	5.3	9	2.2	9
5	Pocahontas #3	VA	Low Vol. Bit.	91	4.4	2	0.7	5
6	Blind Canyon	UT	High Vol. Bit.	81	5.8	12	0.6	5
7	Lewiston-Stockton	WV	High Vol. Bit.	83	5.3	10	0.7	20
8	Beulah-Zap	ND	Lignite	73	4.8	20	0.8	10

The coals are listed in the order collected. The weight % C, H and O values are given on the moisture and ash-free basis, while S and ash are on the dry basis.

The premium quality requires maximal effort to achieve each of several objectives with regard to the handling of the coal. These objectives included minimal oxygen exposure, humidity control, thorough mixing, extensive analysis and long term supplies. Minimal oxygen exposure involved the use of a freshly exposed coal face for the sample, and rapid removal of the sample. The samples were placed in stainless steel drums, sealed and purged with 99.999% argon at the mine site, typically starting within three hours of collection. The samples were sealed in the drums and slightly pressurized for transport to Argonne National Laboratory (ANL) for processing in a unique nitrogen-filled enclosure. This large glove box is about 5-6' wide, 13' tall and would be 40' long if it were built in a straight line. This glove box is operated with 100 ppm of oxygen or less during the processing to protect the samples from atmospheric oxygen. The samples are sealed in glass with this atmosphere. The humidity control is exercised to minimize any moisture loss during the processing. The lack of moisture loss is expected to avoid any damaging effect on the coal pores and retain the properties of the pristine coal as much as possible. The samples are thoroughly mixed in one ton batches in a mixer-blender to provide uniform properties throughout the entire batch. The samples have been extensively analyzed by the Commercial Testing and Engineering Company through a series of more than 50 different laboratories for the proximate and ultimate analyses. About 20% of the ton-sized batch was packaged into sealed glass ampoules containing either 5 grams of -100 mesh or 10 grams of -20 mesh material. This supply seems sufficient to meet current demand levels for about 30 years for the more popular samples and longer for those which are less frequently requested.

CURRENT STATUS AND USAGE

Requests for samples come at an irregular but frequent basis. The shipments to date exceed 12,000 ampoules to more than 256 users distributed over the world. The total number of ampoules which were shipped since January 1986 is shown in Figure 1. The most-requested samples can be seen from Figure 2, which shows the number of ampoules shipped for each of the samples in the order collected.

The inventory of ampoules is such that shipments can continue at the current rate for about 30 years. This would require the filling of additional ampoules to replenish the inventory from 5 gallon carboys which have been prepared for this purpose. The capacity exists to provide about 50,000 of the ampoules of 5 grams of -100 mesh material and 25,000 of the 10 grams of -20 mesh size.

USERS HANDBOOK

The Users Handbook for the Argonne Premium Coal Sample Program (1) has served as the primary document which provides information about the program. This Handbook was initially issued in March 1989 as a 37 page document. It contained a description of the program including the selection, collection, processing and packaging of the samples as well as the analysis and distribution methods. Later sections included analytical information and bib-

liography of references to the work published referring to the samples. Indices by author, subject and journal were included. Finally some safety and ordering information were included.

The popularity of the document and the increasing amount of available information led to the publication of the second edition in October 1989. The amount of analytical information was increased, the bibliography grew to 111 references, a coal index was added and a new literature summary was started. This document had grown to 64 pages. The material appeared also in the form of an Argonne National Laboratory report with the number ANL/PCSP-89/1 which is available through the National Technical Information Service as a referenceable document. Free copies may be obtained on request to the author.

The document is continually growing as the literature references increase in number. At the time of the writing of this paper, (May 1990) there were 178 references in the draft. The authors know of enough additional papers in various stages of review to realize that the number should surpass 200 near the time of presentation of this paper. The analytical information grows as it is reported in the literature and individual investigators supply it to the author. There are over 30 pages of it in the draft. A new paper describing the APCSP has been prepared and is intended to appear in the literature (2) as well as in the future version of the Handbook. This reference can be used by all future authors of papers on research with these samples to facilitate future literature searches, and aid in providing complete bibliographies. A number of papers have already appeared which describe the program and related activities (3,4,5,6,7).

The number of publications and shipments continues to increase. The current ratio of shipments to papers is about two shipments per paper.

QUARTERLY NEWSLETTER

In addition to the Users Handbook a Newsletter is mailed without charge to the recipients of the samples and some individuals who have asked to be on the mailing list. This Newsletter provides information of value to the users and aids in keeping them current on additions to the bibliography which appears in the Handbook.

SYMPOSIA

This paper will be part of a Symposium on Research with Argonne Premium Coal Samples. The Symposium is the fourth in an annual series which have been organized to provide a forum for current work with the samples. The combination of Symposia, Newsletters and Handbooks is intended to provide an efficient and effective means of dissemination of information about the samples.

FUTURE PLANS

The APCSP plans included the development of the capability to offer separated macerals to the coal research community. Limitations on funding brought about by the U. S. budget deficit and

restrictions on support by the Gramm-Rudman bill have led to a postponement of new projects for an indefinite period. This activity will wait until funding is available. It is hoped that separated maceral concentrates from the Lewiston-Stockton sample will be available as a liptinite concentrate, a vitrinite concentrate, and an inertinite concentrate. The large amount of vitrinite in the Illinois #6 sample will lead to an effort to offer not just the three concentrates but also three vitrinite concentrates as low, medium and high density vitrinite.

The Users Handbook will continue to grow as the number of references continues to grow. These will be incorporated in the bibliography. The literature summary cannot be continued as originally envisaged due to limitations on the support for the program and the expertise of the author. Instead efforts are underway to recruit a number of volunteers to participate in the review of the literature and contribute to the Literature Summary section. Recognition of the authors will be included, and the reviews will be reviewed by other individuals for balance and completeness. As the number of pages grows this document will approach the size of a preprint of the Fuel Chemistry Division. The cost of printing and distribution will probably limit publication to an annual basis.

ACKNOWLEDGMENTS:

The author gratefully acknowledges the support of the U. S. Department of Energy, Office of Basic Energy Sciences, Chemical Sciences Division under contract W-31-109-ENG-38.

REFERENCES:

1. Users Handbook for the Argonne Premium coal Sample Program, Karl S. Vorres, ANL/PCSP-89/1, Argonne National Lab.
2. Karl S. Vorres, Energy & Fuels, in press
3. Directions of Research from the Argonne Premium Coal Sample Program, Vorres, Karl S., Coal Science & Technol. 11, 1987 Intl. Conf. on Coal Science, 937-940 (1987)
4. The Eight Coals in the Argonne Premium Coal Sample Program. Vorres, Karl S. and Janikowski, Stuart K., Preprints, Fuel Chem. Div., Am. Chem. Soc. 32 (1) 492-499 (1987)
5. The Preparation and Distribution of Argonne Premium Coal Samples. Vorres, Karl S., Preprints, Fuel Chem. Div., Am. Chem. Soc. 32 (4) 221-226 (1987)
6. Illinois Basin Coal Sample Program and Access to Information on Illinois Basin Coals. Kruse, Carl W.; Harvey, Richard D.; Rapp, David M., Preprints, Fuel Chem. Div., Am. Chem. Soc. 32 (4) 359-365 (1987)
7. Sample Preparation for, and Current Status of the Argonne Premium Coal Sample Program. Vorres, Karl S., Preprints, Fuel Chem. Div., Am. Chem. Soc. 33 (3) 1-6 (1988)

Fig. 1 Total Ampoule Shipments Through April 1990

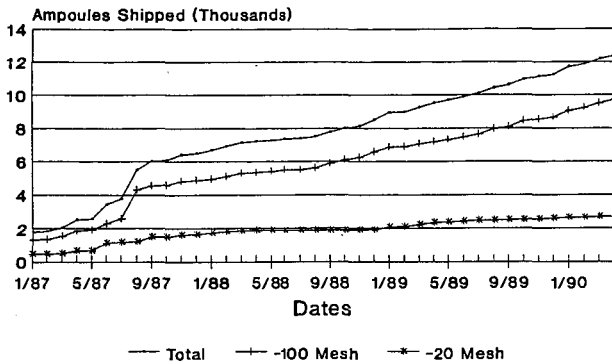
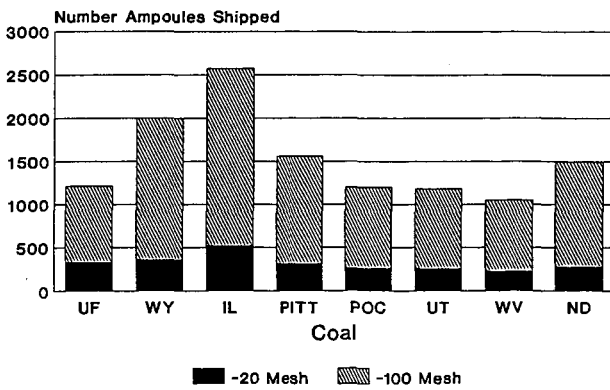


Fig. 2 Number of Ampoules Shipped Through April, 1990



DIRECT DETERMINATION AND QUANTIFICATION OF SULFUR FORMS IN COALS
FROM THE ARGONNE PREMIUM SAMPLE BANK

Martin L. Gorbaty, Graham N. George, Simon R. Kelemen and Michael Sansone
Exxon Research and Engineering Company
Annandale, NJ 08801

Keywords: Organic Sulfur, XANES, XPS, Rank

Sulfur K Edge X-ray Absorption Near Edge Structure Spectroscopy (XANES) and X-ray Photoelectron Spectroscopy (XPS) have been developed for the direct determination and quantification of the forms of organically bound sulfur in nonvolatile petroleum and coal samples. XANES and XPS spectra were taken of a number of model compounds, mixtures of model compounds, heavy petroleum and coal samples. A third derivative analysis of the XANES spectra and curve resolution of the XPS spectra allowed approximate quantification of the sulfidic and thiophenic components of the model mixtures and heavy hydrocarbon resources. Both techniques were used to characterize organically bound sulfur forms in coals from the Argonne Premium Coal Sample Bank and both show a monotonic increase of thiophenic sulfur with increasing rank.

Introduction

X-ray Absorption Near Edge Structure (XANES) Spectroscopy and X-ray Photoelectron Spectroscopy (XPS) are two techniques which have been applied recently for the direct speciation and approximate quantification of organically bound forms of sulfide and thiophenic sulfur in nonvolatile liquid and solid carbonaceous materials (1-5). Both techniques have been used to characterize the levels of sulfide and thiophenic sulfur forms in coals from the Argonne Premium Coal Sample Program and to develop a correlation of sulfur forms with rank.

It is known that organic sulfides can be converted to thiophenes on heating. For example, it has been shown that when benzylsulfide is heated to 290°C, tetraphenylthiophene, hydrogen sulfide and stilbene are produced (6). Extending this to organically bound sulfur forms in coals, it would be expected that the ratio of thiophenic sulfur to sulfide sulfur would increase with increasing rank, as the coal precursor materials experience more and more severe geological temperatures and pressures during metamorphism. Recent data on a number of coals of different rank, obtained by flash pyrolysis experiments (7) which measure and correlate H₂S evolution with level of sulfide sulfur present indicate this trend. However, these experiments leave open the question as to whether sulfur forms are interconverting during the pyrolysis. H₂S evolution may not correlate directly with sulfide sulfur and coupled with heat and mass transport limitation considerations, particularly for solids, it is not unreasonable to question whether at least some of the thiophenic forms observed by pyrolysis techniques are produced during heating. Therefore, the forms of organically bound sulfur in coals of different rank obtained from the Argonne Premium coal sample program were determined by direct measurement using XPS and XANES.

Experimental

The procedures for obtaining XANES and XPS spectra have been discussed elsewhere (1-4). The XANES spectra were recorded at the National Synchrotron Light Source at Brookhaven National Laboratory on line X-10C. To avoid ambient temperature oxidation, sample preparations were done in a glove bag filled

with nitrogen. Coal samples, which were all <100 mesh as-received, were dusted onto mylar tape and the sample holders transported to the beamline in nitrogen filled bottle. Similarly, preparation of samples for XPS were done in a nitrogen filled dry box, and the samples inserted into a fast entry air lock. Fluorescence XANES spectra were recorded using a Stern-Heald-Lytle detector (8). Pyrite interferences in the XANES spectra were removed by subtracting the third derivative spectrum of iron pyrite from the third derivative spectrum of the coals until the lowest energy pyrite "peak" was removed. Pyrite interferences in the XPS data from Illinois #6 coal were removed by subtraction during the curve resolution analysis by the method described previously (3). The accuracy of both the XANES and XPS methods for determining organically bound sulfide and thiophenic sulfur forms is estimated to be $\pm 10\%$.

Results

XANES spectra and their third derivative traces for the 8 Argonne Premium samples are shown in Figure 1. The feature at about 2468.5 eV is associated with pyritic sulfur, that at 2469.8 eV with sulfide sulfur and 2470.4 eV with thiophenic sulfur. After subtracting pyrite interferences, measurement of peak heights from the baselines provided the approximate quantifications of sulfide and thiophenic sulfur forms found in these samples. These data are listed in Table 1 and plotted in Figure 2 against carbon content of the coals. Except for the Illinois #6 data, there is a clear increase in thiophenic sulfur with increasing carbon content of the coals.

XPS data on the same samples are also shown in Table 1 and are plotted in Figure 2. With the exception of Illinois #6 coal, it was possible to curve resolve the organic sulfur 2p spectrum using sulfur species components fixed at 163.3 eV and 164.1 eV for sulfide and thiophenic sulfur respectively. The sulfur signals representative of these single species under the experimental conditions of this and previous studies (4,5) were determined from the instrumental response to pure sulfur model compounds. The signal of a single sulfur species is composed of two peaks representing 2p_{3/2} and 2p_{1/2} components having a 2:1 relative intensity and separated in energy by 1.2 eV. Each component is composed of equally mixed Gaussian and Lorentzian line shapes and a full width-half maximum of 1.4 eV. These conditions were used for all curve resolving procedures. The XPS data confirm the trend of increasing thiophenic sulfur content with increasing rank.

Pyritic sulfur was observed only in the Illinois #6 spectrum. The XPS spectra in the unoxidized region of all other Argonne Premium samples were found not to contain contributions from pyritic sulfur. A weak iron 2p signal was detected in the spectra of Upper Freeport, Pittsburgh #8, Lewiston-Stockton and Beulah-Zap. The levels, when normalized to the carbon 1s signal were lower than expected from bulk elemental analyses. This behavior has been noted before with other coals (3,9). In every case, a broad peak was centered well below 711 eV, indicative of iron oxides or sulfate in poor electrical contact with the organic matrix. No evidence was found for a pyritic iron signal in this study, and on this basis the XPS sulfur 2p spectra were judged to be free of interference effects due to pyritic sulfur.

Discussion and Conclusions

Both XPS and XANES data confirm the trend of increasing thiophenic sulfur content with rank for the coals studied. This is the first such evidence obtained by direct measurement. Figure 3 shows both sets of data plotted

against each other, the solid line being the parity situation. It is seen that the surface and bulk measurements are in good agreement and fall within the established limits of accuracy for both methods. The implication of this is that sulfur distributions at the surface and in the bulk are similar.

The outlying point in Figures 2 and 3 arises from the XANES data of Illinois #6 coal. If there are errors in the pyrite subtraction procedure, or if absorptions of the thiophenic species actually present are shifted due to substituent effects, the values reported herein for thiophenic sulfur in this coal would be low. These possibilities are under study at this writing.

Acknowledgments

X-ray absorption spectra were recorded at the National Synchrotron Light Source (Brookhaven National Laboratory), which is funded by the Division of Material Sciences, U. S. Department of Energy under contract DE-AC02-76CH-00016. The writers wish to thank Dr. K. S. Vorres (Argonne) for providing the samples used in this study, and Mr. P. Kwiatek for carrying out the XPS measurements.

References Cited

- 1) George, G. N.; Gorbaty, M. L. *J. Amer. Chem. Soc.*, 1989, 111, 3182.
- 2) George, G.N.; Gorbaty, M.L.; Kelemen, S.R. In *Geochemistry of Sulfur in Fossil Fuels*; Orr, W.L., White, C.M., Eds.; ACS Symposium Series; American Chemical Society; Washington DC, In press.
- 3) Kelemen, S. R.; George, G. N.; and Gorbaty, M. L. *ACS Div. Fuel Chem. Preprints*, 1989, 34, 729; *FUEL*, 1990, 69, in press.
- 4) Gorbaty, M. L.; George, G. N.; Kelemen, S. R. *ACS Div. Fuel Chem. Preprints*, 1989, 34, 738; *FUEL*, 1990, 69, in press.
- 5) Kelemen, S. R.; George, G. N.; Gorbaty, M. L. *Fuel Process. Technol.* 1990, 24, 425.
- 6) Fromm, E. and Achert, O. *Ber.*, 1903, 36, 545.
- 7) Calkins, W. H., *Energy Fuels*, 1987, 1, 59; Torres-Ordonez, R. J.; Calkins, W. H.; Klein, M. T. In *Geochemistry of Sulfur in Fossil Fuels*; Orr, W.L., White, C.M., Eds.; ACS Symposium Series; American Chemical Society; Washington DC, In press.
- 8) Stern, E; Heald, S. *Rev. Sci Instrum.*, 1979, 50, 1579.
- 9) Perry, D. L.; Grint, A. *Fuel*, 1983, 62, 1029.

Table 1

THIOPHENIC SULFUR INCREASES WITH RANK
(ARGONNE PREMIUM COAL SAMPLES)

COAL	% CARBON (daf Basis)	MOLE % ($\times 10$)	
		BY XANES	BY XPS
BEULAH-ZAP	74.05	46	55
WYODAK-ANDERSON	76.04	58	83
ILLINOIS #8	80.73	47	89
BLIND CANYON	81.32	75	65
PITTSBURGH #8	84.95	77	75
LEWISTON-STOCKTON	85.7	74	88
UPPER FREEPORT	88.08	89	81
POCAHONTAS	91.81	98	100

Figure 1

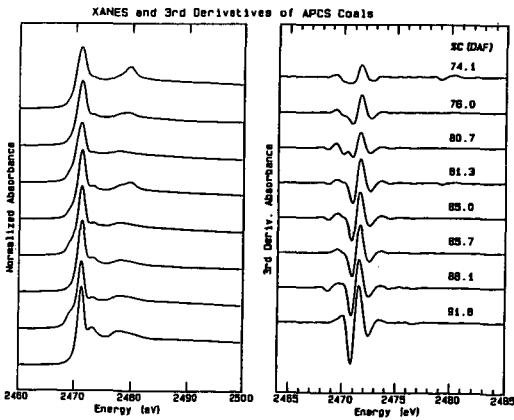


Figure 2

THIOPHENIC SULFUR INCREASES WITH RANK
ARGONNE PREMIUM COAL SAMPLES

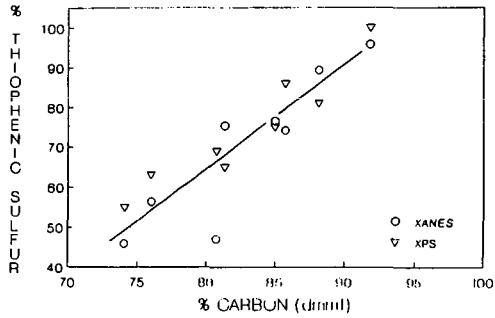
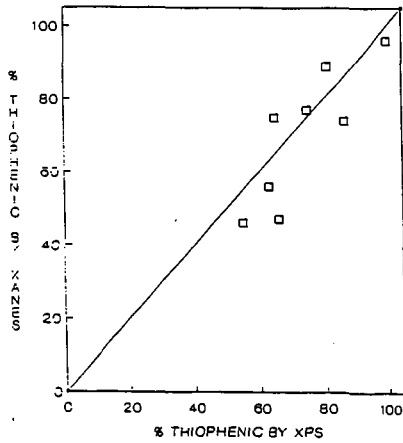


Figure 3

XPS/XANES DATA COMPARISON
(ARGONNE PREMIUM COAL SAMPLES)



COAL MINERALOGY, FORMS OF SULFUR AND IRON, AND COAL LIQUEFACTION PROPERTIES FOR THE ARGONNE PREMIUM COALS AND NINE KENTUCKY COALS.

Naresh Shah, Robert A. Keogh, Frank E. Huggins, Gerald P. Huffman, Anup Shah, Bhaswati Ganguly, and Sudipa Mitra, 233 Mining and Mineral Resources Bldg., University of Kentucky, Lexington, KY 40506.

Keywords: Sulfur XAFS spectroscopy, ⁵⁷Fe Mössbauer Spectroscopy, Computer Controlled Scanning Electron Microscopy (CCSEM)

The eight Argonne Premium coal samples, augmented by nine Kentucky coals, were selected for this study of the relationship of mineral parameters and liquefaction behavior. Kentucky coals were screened from many coals as they exhibited high, low and intermediate values of rank, sulfur content and liquefaction yields. Table 1 lists the selected Kentucky coals and their carbon and sulfur analyses.

Liquefaction

Liquefaction experiments were carried out on all coals at 385 C with tetralin as solvent (1:1.5 coal/solvent ratio) and without any catalyst [1]. Microautoclaves (tubing bombs) were cold pressurized to 800 psi with hydrogen before heating to reaction conditions. Products of liquefaction were classified as: oils - pentane soluble; asphaltenes - pentane insoluble, benzene soluble; preasphaltenes - benzene insoluble, pyridine soluble; insoluble organic matter (IOM) - pyridine insoluble. Total conversion is defined as 100-IOM. Figure 1 is the bar chart showing the results of liquefaction reactions for all coals.

CCSEM

The mineral and inorganic species can act as catalysts or poisons during liquefaction depending on reaction conditions. It is, therefore, important to know the types of minerals present and how they are distributed in coal. Computer controlled scanning electron microscopy (CCSEM) is an excellent tool to rapidly characterize mineralogical information of coals [2]. Tables 2 and 3 list the mineralogical data obtained to date by CCSEM examination of Argonne and Kentucky coals. Two of the Argonne coals remain to be analyzed. With CCSEM, we can also determine average sizes and size distributions of the various minerals present in the coal. We are currently trying to correlate the pyrite surface area to the liquefaction conversion percentages.

It may be noted that "mixed silicates" account for a fairly large percentage of the mineral matter in these raw coal samples. This phase primarily includes clay minerals and quartz in juxtaposition to each other, perhaps in partings. This is illustrated by the ternary diagram in Figure 2. Here, each point represents a mineral feature identified in the CCSEM analysis that contains $\geq 90\%$ of $(K + Fe) + Al + S$ on the basis of its energy dispersive X-ray (EDX) spectrum. The composition is normalized to these four elements and plotted in a ternary representation, as shown. It is evident that there is a range of compositions extending between the quartz, kaolinite, and illite composition areas. It is these intermediate compositions that the coal mineral analysis (CMA) program identifies as mixed silicates.

Mössbauer Spectroscopy

Mössbauer spectroscopy is used to identify and quantify iron bearing phases present in the coals. [3,4]. Iron predominantly exists as pyrite, siderite or Fe-containing clay in coals. Mössbauer spectroscopy is the most accurate tool to quantify pyrite in coal and by using simple stoichiometric formula we can obtain the pyritic sulfur content of the coal. Table 4 lists the Mössbauer spectroscopy results for all coals. As it is clearly evident, the Argonne coals were in pristine condition and do not exhibit any pyrite oxidation.

However, some of the Kentucky coals, mainly those with high pyrite contents have undergone some minor oxidation that converts pyrite to sulfate form.

In order to examine the transformations of Fe-bearing minerals in coals as they undergo liquefaction and thereby assess the role of the inherent iron minerals as catalysts, the insoluble organic matter (IOM) of the Argonne Premium Sample coals were also investigated using Mössbauer spectroscopy. Figure 3 shows room temperature Mössbauer spectra of Illinois #6 coal before and after liquefaction treatment. In Illinois #6 coal, almost all Fe is present in the form of pyrite; after the liquefaction test, about 60% of the pyrite converts to pyrrhotite, while the remaining pyrite is unconverted. Under more severe conditions and/or longer periods of time, all of the pyrite would convert to pyrrhotite. In the Pocahontas #3 coal, iron is distributed among clays, siderite, and pyrite; however, in the Pocahontas #3 IOM, Fe in clays and carbonate remains unchanged whereas pyrite has been converted to pyrrhotite. As summarized in the Table 5 for the Argonne Premium Samples, this observation appears quite general: the Fe-bearing minerals, other than pyrite, do not appear to undergo significant transformation during liquefaction, whereas, some or all of the pyrite converts to pyrrhotite. It is likely that only Fe in the form of pyrrhotite is the primary catalytic species. Fe in the coal present in the form of clays is likely to be inactive.

Sulfur XAFS

It can be expected that different sulfur forms will behave differently under the same process conditions during liquefaction conditions and so it is important to identify the presence and reactions of each sulfur form under different conditions. The combination of Mössbauer and XAFS spectroscopy provides a unique approach to focus on both the different organic and inorganic forms of sulfur [5]. Figure 4 shows the sulfur K-edge XANES of three Argonne coals with pyrite removed. All three spectra are quite similar to each other indicating that the forms of sulfur present after pyrite removal are essentially the same in the three different coals. From our previous studies, we can assign various peaks in sulfur XANES to various forms of sulfur present in coals as follows: sulfidic sulfur (peak at 1.6 eV), thiophenic sulfur (peak at 2.6-2.8 eV), sulfoxide (peak at 4.5 eV), sulfone (peak at 9 eV) and sulfate (peak at 11 eV). We are currently trying to quantify the forms of sulfur present in these coals by curve fitting various features of the spectra and comparing the results to the data from standards.

REFERENCES

1. R.A. Keogh, B.H. Davis, *J. Coal Quality*, 7(1), (1988), 27.
2. F.E. Huggins, G.P. Huffman, *Analytical methods for coal and coal products*, Vol. III, Chapter 50, Ed. K.Vorres, (1981), 371.
3. F.E. Huggins, G.P. Huffman, R.J. Lee, *ACS Symposium Series*, 205, (1982), 239.
4. G.P. Huffman, F.E. Huggins, *Fuel*, 57, (1978), 592.
5. G.P. Huffman, F.E. Huggins, S. Mitra, N. Shah, R.J. Pugmire, B. Davis, F.W. Lytle, R.B. Gregor, *Energy and Fuels*, 3, (1989), 200.

Table 1. Rank and total sulfur content of selected Kentucky coals

UKCAER Coal #	Seam	County	%C DAF	%S DAF
91864	WKY #9	Union	82.15	3.93
6398	Horton	Horton	85.33	0.86
2145	Peach Orchard #3	Magaffin	83.66	0.63
71302	WKY #6	Caldwell	82.50	3.37
3913	Stockton	Martin	82.34	0.75
2167	Cannel City	Magaffin	80.97	1.62
5416	Beaver Creek	Pulaski	74.45	13.92
71464	WKY #9	Henderson	79.44	3.84
71468	WKY #9	Muhlenberg	80.27	4.15

Table 2. Mineral Composition of Six Argonne Coals

Mineral Species	Wt% of Mineral Matter					
	Up. Fr.	Ill #6	Pitt #8	Poca #3	Bl. Cany	Lew Stoc
Quartz	5	9	12	4	4	10
Kaolinite	9	3	8	10	9	15
Illite	35	18	19	8	36	48
K-feldspar		<1		<1		
Chlorite	1			4		
Montmorillonite		<1	<1	<1	1	
Misc. Silicates	17	23	26	34	41	25
Pyrite	25	27	25	4	3	1
FeSO4					<1	
Gypsum	<1					
Chalcopyrite	<1			1		
Misc. Sulf.	1	1	1	<1	<1	<1
Halite (NaCl)				<1		
Apatite			<1			
Misc. Phosphates				<1		<1
Fe-rich		<1		<1	<1	<1
Calcite		8	1	7	2	
Ankerite				<1		
Mixed Carbonates	1	1	<1	5	1	<1
Ti rich		1	1	<1		1
Trace-rich	<1					
Qtz-Sulfur		1	<1			
Qtz-Pyrite	<1	<1		<1		
Sil-Sulfur	<1	3	2		<1	
Sil-Pyrite	<1	1	<1			
Al-rich				3		
Misc. Mixed	2	3	4	15	3	<1

Table 3. Mineral Composition of Kentucky Coals

Mineral Species	Wt% of Mineral Matter								
	6398	71468	2145	71302	3913	91864	2167	5416	71464
Quartz	3	8	11	7	10	13	6	1	8
Kaolinite	12	4	7	3	8	3	2		7
Illite	5	17	43	21	27	16	21	1	12
K-feldspar		<1		1	<1	1	1		
Chlorite	<1		<1	<1			1		
Montmorillonite	1		<1		<1	<1	<1		<1
Misc. Silicates	57	20	36	27	50	22	30	6	27
Pyrite	2	31		26		26	6	55	27
FeSO4		<1		<1		<1	<1	1	<1
Jerosite								1	
Gypsum									
Chalcopyrite									
Misc. Sulf.	<1	1		4	1	5	1	13	3
Halite (NaCl)									
Apatite							<1		
Misc. Phosphates									
Fe-rich	1						14	<1	
Calcite	1	11				<1			4
Ankerite									
Mixed Carbonates	1	1	<1			<1	11	<1	<1
Ti rich	3	<1	<1		<1	<1		<1	<1
Trace-rich			<1						
Qtz-Sulfur		<1		<1		1		1	1
Qtz-Pyrite		<1		3		1	<1	6	<1
Sil-Sulfur	5	3		2	2	5		2	5
Sil-Pyrite	<1	1	<1	2		1	<1	7	1
Al-rich						<1			
Misc. Mixed	10	3	1	5	2	5	7	6	5

Table 4. Mössbauer Data for Argonne Premium and Selected Kentucky Coals

Argonne Premium or Kentucky coals	Wt% pyritic sulfur	%Fe in			
		Clay	Siderite	Pyrite	Sulfate
Upp. Freeport	1.60	6	0	94	
Wyodak	0.13	0	26	74	
Illinois #6	2.14	3	0	97	
Pittsburgh #8	1.26	1	0	99	
Pocahontas #3	0.11	33	46	20	
Blind Canyon	0.25	0	28	72	
Lewis-Stockton	0.20	32	15	53	
Beulah-Zap	0.22	0	0	100	
91864	2.04			95	5
6398	0.03	61	16	22	
2145	0.15	57		43	
71302	1.86	5		88	7
3913	0.17	34		66	
2167	0.93	9	72	19	
5416	11.50			92	8
71464	1.87			96	4
71468	2.14			95	5

Table 5. Mössbauer Data for Argonne Coal IOMs

Argonne Premium Coal	%Fe in			
	Clay	Siderite	Pyrite	Pyrrhotite
Upper Freeport				100
Wyodak		21	42	37
Illionis #6			40	60
Pittsburgh #8			33	67
Pocahontas #3	38	50		12
Blind Canyon		31		69
Lewis-Stockton	32		31	37
Beulah-Zap			31	69

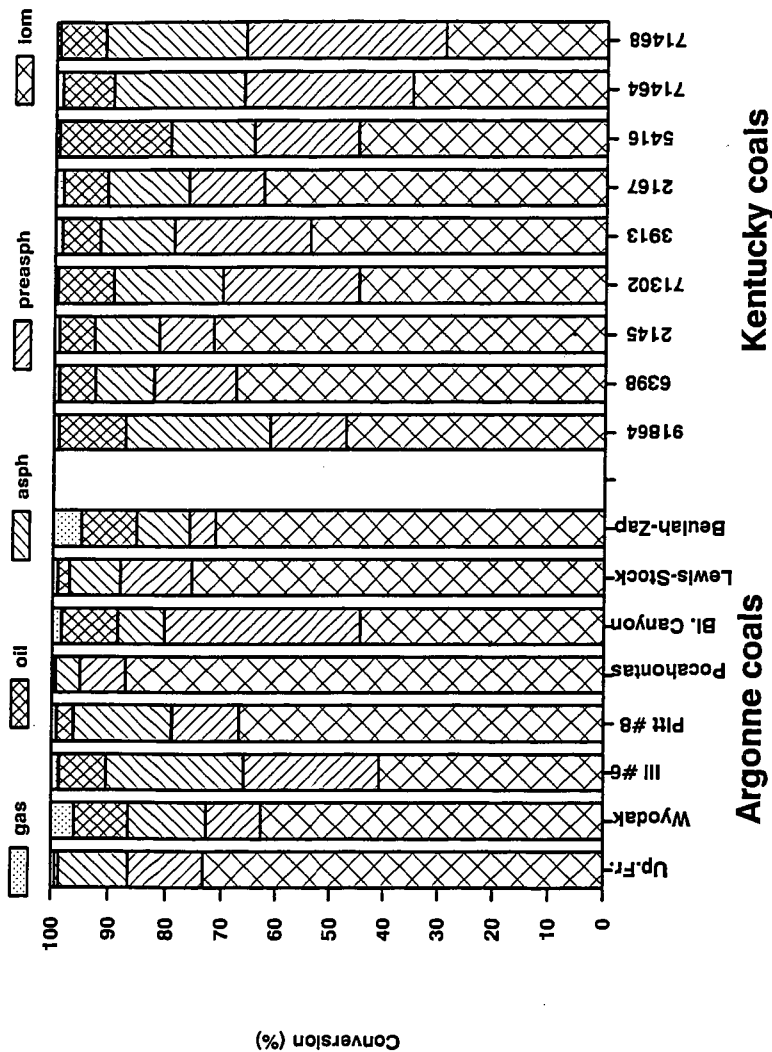


Figure 1. Liquefaction conversion percentages for Argonne Premium Coals and Kentucky Coals.

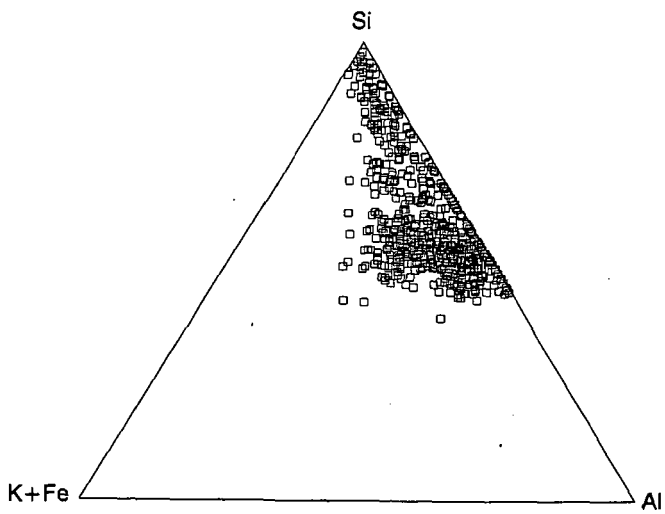


Figure 2. Ternary presentation of compositional data for quartz and clay minerals in Kentucky coal #3913.

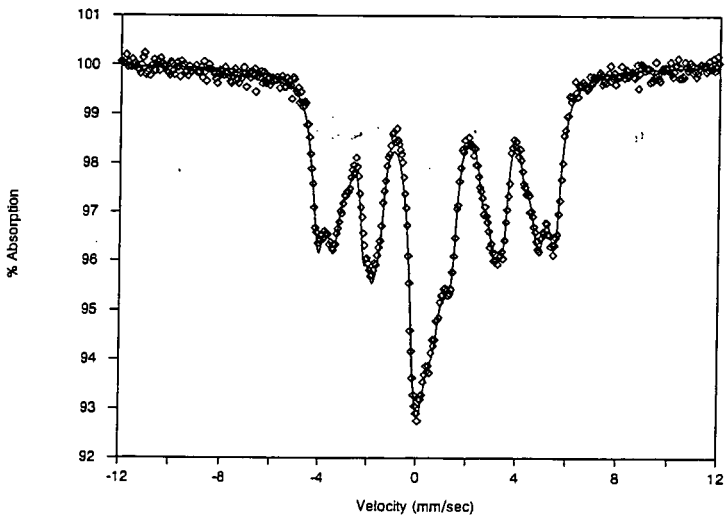
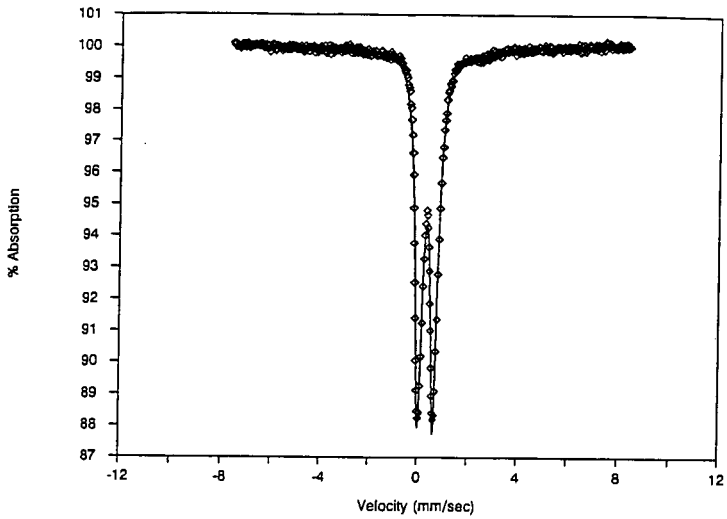


Figure 3. Mössbauer spectra of Illinois #6 raw coal (Top) and IOM (Bottom)

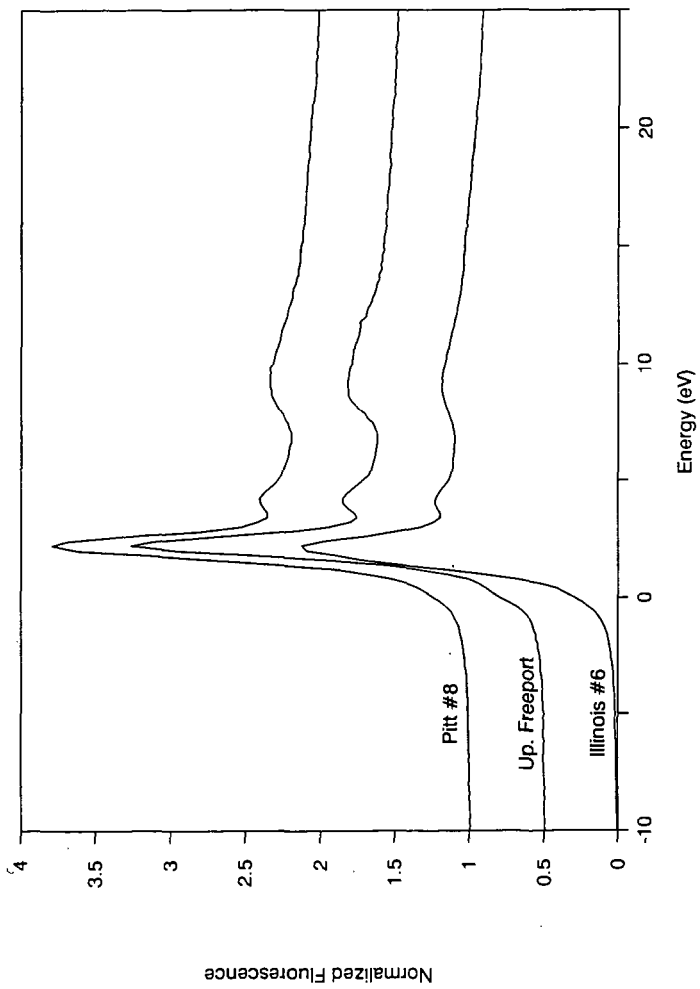


Figure 4. Sulfur K-edge XANES of three Argonne coals with pyrite removed.

SULFUR-PROMOTED METAL OXIDES AS COAL LIQUEFACTION CATALYSTS

Vivek Pradhan, J. W. Tierney and Irving Wender

Department of Chemical and Petroleum Engineering
University of Pittsburgh
Pittsburgh, PA 15261

Keywords: Catalysis, Sulfated Iron and Tin Oxides, Coal Liquefaction

ABSTRACT

This paper reports an investigation of the activities of iron and tin oxides treated with varying amounts of sulfate for the direct liquefaction of a bituminous coal (Illinois No. 6 from the Argonne Premium Coal Sample Bank). The work described here also attempts to correlate the physico-chemical properties of the sulfate-promoted oxides before the reaction and the types of active phases formed under liquefaction conditions with their apparent activities for hydrocracking of coal. $\text{Fe}_2\text{O}_3\cdot\text{SO}_4^{2-}$ was found to be an effective catalyst for coal liquefaction even when used in small concentrations (<0.7 wt % iron). It resulted in an 86 wt % (maf basis) conversion of Illinois No. 6 coal at 400°C and 1000 psig hydrogen (initial); more than 50 wt % of the products consisted of oils (n-pentane solubles). Addition of elemental sulfur to the same catalyst (at 0.35 wt % Fe) enhanced the overall conversion to 90.3 wt % with more than 60 % of products consisting of oils. Similar results for coal conversion were obtained for a solid superacid made from tin, $\text{SnO}_2\cdot\text{SO}_4^{2-}$. These conversions were much higher than those obtained in a thermal run under the same reaction conditions (% conversion = 52 %, wt % oils = 16). For both iron and tin oxides, sulfated forms containing between 1.5 wt % to 6 wt % of SO_4^{2-} group on the surface were more active than their respective unsulfated forms. Promotional effects of sulfate group are believed to be due to an increase in "catalyst-dispersion" and surface acidity.

INTRODUCTION

Catalysts in highly dispersed form are believed to be very active for conversion of coal to liquids via direct coal liquefaction.^{1,2,3} Understanding the effects of catalyst dispersion (catalyst surface area per mass) and composition on catalyst performance is still far from complete. In direct coal liquefaction, the supported metal catalysts such as Co-Mo/ Al_2O_3 may suffer from poor contact with the feed and rapid deactivation.⁴ Unsupported dispersed catalysts derived from finely divided solid precursors offer efficient contact of coal-solvent slurries with catalyst surfaces. Addition of a low surface area solids requires high catalyst concentrations.⁵ Particulate pyrite (FeS_2) with average particle size of several microns is not very effective at low catalyst concentrations. A catalyst with a high specific surface area and fine particulate size can be utilized even at very small concentrations⁶ for achieving better performance in terms of overall coal conversion and selectivity to lighter products (oils) in direct coal liquefaction. A cheap disposable catalyst such as iron is highly desirable.

High dispersions of catalysts have been obtained by different methods such as the impregnation technique³, use of water-soluble¹ or oil-soluble precursor², and use of finely divided powders.⁹ All these methods allow the formation of finely dispersed active inorganic phases under reaction conditions. Maximum interaction of coal, vehicle, and H_2 can occur on the catalyst surface with a highly dispersed catalyst. One method of increasing dispersion of a catalyst is to introduce it as a very finely divided solid

(average particulate size of a few nanometers) to the coal-solvent reaction mixture. Such finely divided powdered precursors are believed to achieve good distribution throughout the coal-solvent slurry and are converted to active inorganic sulfide phases. The high dispersions of active phases thus achieved is believed to allow the use of catalyst concentrations below 1.0 wt % with good performance.¹⁰

We chose to study the catalytic activity of sulfate-treated iron and tin oxides and its relation to catalyst properties. These oxides have been claimed to be "superacidic"^{11,12} as have the oxides of other transition metals such as Ti, Zr, Hf. These oxides have a Hammett acidity function, $H_0 < -12.0$ and catalyze a variety of hydrocarbon transformations at low temperatures.¹² It is believed that the bidentate sulfate group on the oxide surface increases its acidity. It is also known¹³ that the sulfate anion prevents sintering of ceramic oxide powders during calcination, thereby reducing the degree of crystallinity and lowering the average crystallite size of these oxides. It was reported first by Tanabe et al.^{14,15} that a sulfate-promoted iron oxide ($Fe_2O_3 \cdot SO_4^{2-}$), claimed to be a solid superacid, was active for promoting C-C bond cleavage in coals and therefore for the hydrocracking of a bituminous Akabira coal (% C = 83.0) at 400°C and under 1000 kg/cm² of H₂. A sulfated iron oxide with about 2 wt % sulfate group (SO_4^{2-}) on its surface was found as active as a well known hydroprocessing catalyst CoO-MoO₃-Al₂O₃. The iron oxide in its sulfated form gave about 75 wt % coal conversion (with 31 % "oils") as compared to unsulfated iron oxide which resulted in only 60 wt % coal conversion with 20 % of "oils". Later work reported by Kotanigawa et al.¹⁶ mentions the use of sulfate-treated iron oxide for some model compound reactions and for direct coal liquefaction reactions. They attributed higher activity of the sulfate-promoted iron oxide to the possible synergism between sulfate (S^{6+}) and sulfide (S^{2-}) phases of iron formed under coal liquefaction conditions. Mariadassou et al.^{17,18} have reported the use of finely divided iron oxides/oxyhydroxides (avg. particle size = 50 nm) such as FeOOH, FeOOH-Al₂O₃ sulfided *in situ* by addition of CS₂ for the hydroliquefaction of a high volatile bituminous coal. They observed an increase in the activity of iron sulfide with decrease in the particle size of iron oxide added as precursor. They also reported that sintering of the oxide particles at high temperatures of coal liquefaction was inhibited by the textural promoter effects of coal. The same group recently reported the activity of finely divided tin oxide-sulfur systems for coal liquefaction.

EXPERIMENTAL

Chemicals: Illinois No. 6 hvB bituminous coal ground to below 100 mesh (<120 μm) was obtained in ampules and under N₂ storage from the Argonne Sample Bank and used as received. Tetralin (99+% pure) was obtained from the Fisher Scientific Co. Illinois No. 6 coal contained 4.8 % sulfur of which 46 % was organic and 54 % was pyritic. It had a composition of 77.7 % C, 5.0 % H, 13.5 % O, 4.8 % S, and 15.5 % ash. The starting materials used for the catalyst preparation were iron alum, urea, 28 % ammonia water which were purchased from the Aldrich Chemical Co. and tin(IV)chloride and iron(III)nitrate were purchased from the Strem Chemical Co.

Catalyst Preparation and Characterization: The sulfate treated oxides of iron and tin were prepared starting from their respective sulfate or chloride salts precipitated with either ammonia water or urea. Both homogeneous as well as heterogeneous coprecipitation routes were followed to prepare the intermediate oxyhydroxides of iron and tin. These oxyhydroxides were then treated with sulfuric acid in varying concentrations. The resultant powders were then dried and calcined at appropriate temperatures. The preparation conditions of these catalysts are indicated in Table 1. The catalysts thus prepared were characterized by various techniques such as BET-surface area analysis, sulfur analysis, thermogravimetry (TGA), X-ray diffraction, and electron microscopy. A Phillips X-ray Diffractometer using Cu-Kα radiation at 30 kV and 25 mA was used to obtain the powder diffraction patterns of the catalysts.

Table 1. Summary of Preparation Conditions of Sulfate Treated Metal Oxides

Cat.Code	Catalyst	Starting Salts	Norm. H ₂ SO ₄	Calcination, T°C
FeCat1	Fe ₂ O ₃	Fe(NO ₃) ₃	-	500
FeCat4	Fe ₂ O ₃ SO ₄ ²⁻	Fe(NO ₃) ₃	1.0	500
FeCat7	Fe ₂ O ₃ SO ₄ ²⁻	Fe Alum*	-	500
FeCat8	Fe ₂ O ₃ SO ₄ ²⁻	Fe Sulfate	-	700
SnCat1	SnO ₂	SnCl ₄ ·5H ₂ O	-	600
SnCat3	SnO ₂ SO ₄ ²⁻	SnCl ₄ ·5H ₂ O	1.0	600
SnCat5	SnO ₂ SO ₄ ²⁻	SnCl ₄ ·5H ₂ O	6.0	600

* Urea was used as a precipitating agent in this preparation.

Average crystallite sizes were calculated from line broadening of the peaks, corrected for instrumental broadening. A Cahn electrobalance was used for thermogravimetric analyses and acidity measurements of catalysts. Transmission electron microscopy (TEM) and scanning electron microscopy (SEM) were carried out for structural investigation of the catalysts using JEOL 35 CX SEM and JEOL 200 CX TEM models. The residues of coal liquefaction experiments were also analyzed using X-ray diffraction and a JEOL 2000 FX STEM (100 kV beam) with an energy dispersive X-ray spectrometer. For the composition and dispersion information about the catalytic phases formed under liquefaction conditions.

Reaction Studies: Direct coal liquefaction experiments were carried out in a 300 ml stainless steel autoclave (Autoclave Engineers) agitated by a turbine impeller and heated by a tube furnace. Illinois No. 6 coal (10 g), tetralin (40 g), and 0.35 or 0.7 wt % Fe or Sn (added as their respective sulfate-treated oxides) were mixed first manually in a beaker and then placed into the reactor, which was flushed with helium and pressurized with 1000 psig hydrogen at room temperature. Stirring was started at room temperature to allow for hydrogen dissolution in the coal-solvent slurry and proper mixing of the reactants. After about 30 minutes, the reactor was heated with furnace heater to 400°C in approximately 35-40 minutes, and held at that temperature for 60 minutes while stirring about 1400 rpm. The reactor was then cooled to below 300°C in about five minutes. Soxhlet extraction with CH₂Cl₂ was used to determine the coal conversion. Soluble products were recovered by rotary evaporation at 45°C under vacuum. Pentane solubles (oils) were determined by adding 40 volumes of n-pentane to CH₂Cl₂ solubles and using Soxhlet extraction with n-pentane. Pentane-insoluble but CH₂Cl₂ soluble material was referred to as asphaltenes. Methylene chloride insolubles (residues) were recovered and stored for further characterization.

RESULTS AND DISCUSSION

Catalyst Characterization: The iron and tin oxides treated with different amounts of sulfate were characterized by the different techniques mentioned above. Interestingly, the average crystallite size of the oxide particles was found to decrease upon treatment with 2 to 6 wt % sulfate anion. A distinct broadening of the X-ray diffraction peaks was observed for these oxides with the increasing sulfate group loadings. At the same time a corresponding increase in the specific surface areas of these oxides was observed when liquid nitrogen physisorption was carried out on the catalysts for determining the surface areas using the BET equation. A linear relationship was observed between the concentration of sulfuric acid used for sulfate treatment and the final amount of SO₄²⁻ group that remained on the surface. The decrease in the crystallite size can be explained if we hypothesize that a bulky sulfate group on the surface of the intermediate oxyhydroxide particles prevents the agglomeration or sintering of the oxide particles

at high temperature. It also probably delays crystallization. Evidence for acidity enhancement of these oxides upon the sulfate-treatment was also observed from pyridine adsorption experiments carried out using a Cahn electrobalance. From X-ray diffraction studies for iron oxides, α - and γ - Fe_2O_3 were found out to be the most abundant crystalline phases, while for tin oxides, the most abundant phase was crystalline SnO_2 . Catalyst characterization results are listed in Table 2. The values of onset liquefaction temperatures of Illinois No.6 coal using different sulfate-treated oxides as catalysts have also been listed in this table. These temperatures were determined using a high pressure, high temperature polarizing light microscope with flowing hydrogen at 300 psig pressure.

Table 2. Effect of Sulfate Loading on Surface Area [S_g] and Crystallite Size [D_{average}]

Cat.Code	Wt % SO_4^{2-}	S_g , m ² /g	XRD: D_{avg}	TEM : D_{avg}	Onset* L.T., °C
FeCat1	0.0	26.82	46 nm	60-70 nm	415
FeCat7	3.4	81.72	16 nm	20-25 nm	410
FeCat4	6.1	79.50	12 nm	20-30 nm	400
SnCat1	0.0	60.50	19 nm	—	410
SnCat3	1.8	97.48	9 nm	15-20 nm	395
SnCat5	3.9	146.23	5 nm	10-15 nm	385

* Onset liquefaction temperature for a thermal run was about 450°C.

As seen from this table, the average crystallite sizes determined for both the sulfated and unsulfated iron and tin oxides based on the X-ray line broadening agree fairly well with those determined with transmission electron microscopy (TEM) using the bright field. Scanning electron micrographs of these catalyst samples were also taken to determine their particle size distribution and surface structure morphology. It was found from both the TEM and SEM images that sulfate-treated iron oxide consists of a bimodal-type distribution of crystallites, with some crystals being rod-like while other are plate-like. The average crystallite size was about 20 nm. Sulfate-treated tin oxides have a porous structure with a sausage-like surface morphology. Their average crystallite size was found to be 15 nm.

Reaction Studies: The coal liquefaction reactions were carried out in a 300 ml stainless steel autoclave. Initially a thermal run was carried out to determine the catalytic activities of the mineral matter (especially pyrite) inherent to coal, i.e., without addition of any external catalyst. This resulted in 52 wt % (maf) total conversion of Illinois No.6 coal, with about 16 wt % n-pentane solubles (oils). The total coal conversion values are calculated based on the weight of the final residue. The sulfate-treated iron and tin oxides were then used in very small concentrations for the liquefaction reactions. One of the iron oxides, Fe Cat 4 (wt % sulfate = 6.1) resulted in a substantially high coal conversion of 86 wt % with 39 wt % conversion to n-pentane solubles. A comparative experiment with Fe Cat 1, which did not contain any sulfate group gave 74 wt % total conversion and 23 wt % conversion to oils. Less than 0.7 wt % Fe was used with respect to coal in these experiments. Similar experiments were run with tin oxides treated with sulfate to determine their efficacy for direct coal liquefaction reactions and to determine the promotional effect of the sulfate group on the activity of the oxides. About 0.8 to 0.9 wt % of tin was used in these runs with respect to coal. Two bar-charts demonstrating conversions and product-distributions for different oxide catalysts based on iron and tin are shown in Figure 3.

As can be seen from the bar-charts in Figure 1, addition of 0.7 wt % Fe in the form of oxide to the reaction mixture enhances total coal conversion as well as conversion to lighter oils. Both sulfate-treated oxides of iron, Fe Cat 4 and Fe Cat 7, were found to increase the total conversions to 86 % and 79 % respectively as compared to 74 % obtained with Fe_2O_3 alone (unsulfated form). Importantly, the amounts

of oils increased from about 23 % for Fe_2O_3 alone to about 38 to 40 % for $\text{Fe}_2\text{O}_3\cdot\text{SO}_4^{2-}$ catalysts. Promotional effects of sulfate groups on catalytic activities of oxides for coal liquefaction were seen for sulfate-treated tin oxides as well. As seen in Figure 1, Sn Cat 5 (wt % sulfate=3.9) resulted in about 85 % total coal conversion with more than 40 % of the products consisting of oils. These values were again higher than those obtained for the unsulfated SnO_2 , which gave 72 % total coal conversion with 32 % oils. A run was also made using iron oxide prepared directly from ferric sulfate by calcination at 700°C (Fe Cat 8). It resulted in about 80 % total coal conversion with 32 % conversion to oils. Some reactions were made at much reduced wt % of Fe and Sn but in the presence of an elemental sulfur added to the reaction mixture. The amount of sulfur added was enough (about 1.1 times the quantity that is required for complete sulfidation of added Fe as $\text{Fe}_2\text{O}_3\cdot\text{SO}_4^{2-}$) to bring about complete *in situ* conversion of oxides to sulfides.¹⁹ Fe Cat 1 and Fe Cat 7 were used separately with the added sulfur. The amount of catalyst was 0.35 wt % with respect to coal. As shown in the Figure 1, total conversions as high as 90+ % were obtained with both the sulfated (Fe Cat 7) and the unsulfated (Fe Cat 1) forms of iron oxides, but the former catalyst resulted in higher conversion to oils (47 % than the latter one (28 % oils). This suggests that the non-stoichiometric iron sulfides (detected later by XRD) formed from sulfate-treated iron oxide were more active for the conversion of asphaltenes to lighter oils than those formed from unsulfated oxide (Fe_2O_3). Comparison of two runs, one with Fe Cat 7 (0.7 % Fe) and other with Fe Cat 7 + S (0.35 % Fe), shows an enhancement in conversion levels (Figure 3). Elemental sulfur was used with one of the sulfated tin oxide for coal liquefaction (wt % Sn=0.4), but no significant effect on conversion was observed. The enhancements in total conversions as well as conversions to oils obtained with sulfate-treated oxides over the unsulfated ones might be attributed mainly to the enhanced "dispersions" (surface area/gm) of the oxides upon the sulfate treatment. Due to increase in the specific surface area and decrease in the average particle size of the oxides upon the addition of small amounts of the sulfate group, the conversion of oxides to active catalytic sulfide phases, especially non-stoichiometric sulfides for iron, is facilitated.¹⁹ (Pyrrhotite, a non-stoichiometric sulfide of iron, is a semiconductor. One wonders whether this property of pyrrhotite has any bearing upon its catalytic activity for coal liquefaction.) More of the active catalyst surface of these sulfides probably becomes available for reaction.

Product Characterization: The CH_2Cl_2 insolubles (residues) recovered from the coal liquefaction reactions were analyzed to determine the composition of metal-sulfide phases formed under coal liquefaction conditions. X-ray diffraction was carried out on these residues to determine their composition and the particle sizes of the inorganic phases formed. Residues recovered from the reactions which employed sulfate-treated iron oxides invariably showed the presence of non-stoichiometric iron sulfides (pyrrhotites) as the major constituent along with traces of FeOOH and Fe_3O_4 . The average crystallite size of the pyrrhotite formed was found to be about 25 to 30 nm. Autoclave runs with sulfate-treated tin oxides resulted in residues rich in SnS with a small amount of pyrrhotite formed by the decomposition of pyrite in coal. These tin sulfides were found to have an average crystalline diameter of about 30 nm. A run was also made with one of the iron oxides (Fe Cat 7) in the presence of activated carbon instead of coal to characterize the dispersions using scanning and transmission electron microscopy (STEM). Some of the liquefaction residues were also characterized using STEM and energy dispersive microanalysis (EDX) and found to contain well dispersed iron-containing particles with particle sizes ranging between 10 to 100 nm. A typical TEM-mode image of iron-containing particles on activated carbon and the X-ray microanalysis are shown in Figure 2. This TEM-image shows a distribution of fine iron-containing particles over the activated carbon support. The EDX spectrum of one of the liquefaction residues indicates the presence of both Fe and S in these fine particles. Further detailed investigation of these liquefaction residues by Mossbauer spectroscopy and EXAFS is in progress.

The composition of CH_2Cl_2 solubles was determined by elemental analysis which was performed by Galbraith Laboratories Inc. (Table 3). Methylene chloride solubles consisted of a mixture of recovered tetralin (GC-analysis) (about 50 wt %, H/C=1.2), naphthalene (about 35 wt %, H/C=0.8) and soluble products from coal (about 15 wt %).

Table 3. Elemental Analysis of CH_2Cl_2 Solubles Obtained from Liquefaction Reactions Employing Different Catalysts

Analysis by Wt % as Received						
Catalyst	% C	% H	% N	% S	% O	{H/C}atom
Thermal	83.97	6.37	1.85	1.23	6.76	0.91
FeCat4	84.69	7.68	<0.50	0.084	0.74	1.09
FeCat1	88.98	8.94	1.30	0.21	1.09	1.20
FeCat7	86.25	8.47	<0.50	0.28	1.25	1.18
SnCat3	87.94	8.80	<0.50	0.24	1.32	1.20
SnCat5	87.44	9.10	<0.50	0.25	1.07	1.25

All the iron and tin oxides used as catalysts for the reaction under the same conditions yielded CH_2Cl_2 solubles with an enhancement in H/C ratios (about 1.2) along with a significant heteroatom removal. This could be due to the increased acidic character of these oxides. A very small amount of both nitrogen (Wt % < 0.5) and sulfur (Wt % < 0.28) was obtained in the solubles from almost all the catalytic runs. From these results, both iron and tin oxides (after transformation into their respective active sulfide phases) seem to function as good hydrogenation and hydrogenolysis catalysts.

CONCLUSIONS

Our experimental work on sulfate-treated metal oxides has shown that the sulfate group immobilized on the surface of these oxides helps increase its surface acidity and promotes the catalytic activity of these oxides for direct coal liquefaction reactions, probably by causing reduction in their average particle diameter and subsequent increase in the specific surface area available for catalysis. The sulfate-treated iron and tin oxides resulted in better coal conversions and product slates than the unsulfated oxides. It appears that finely divided sulfate-treated oxides are effective for overall coal conversion as well as the conversion of the asphaltenes to lighter oils. The oxides seem to convert themselves in to their respective metal-sulfides with nano-size particles (10 to 100 nm), which is an indication of good catalyst-distribution during coal liquefaction reaction. These sulfate-treated oxides of iron and tin also seem to function as better hydrogenolysis catalysts for hydrodesulfurization and hydrodenitrogenation reactions.

ACKNOWLEDGEMENTS

The authors gratefully acknowledge the contributions of Cole van Ormer and Dr. W. Soffa for the TEM work and George McNaumus and Dr. J. R. Blachere for the SEM and STEM work. Funding support from the U.S. Department of Energy under grant number DE-FG22-87PC79928 is gratefully acknowledged.

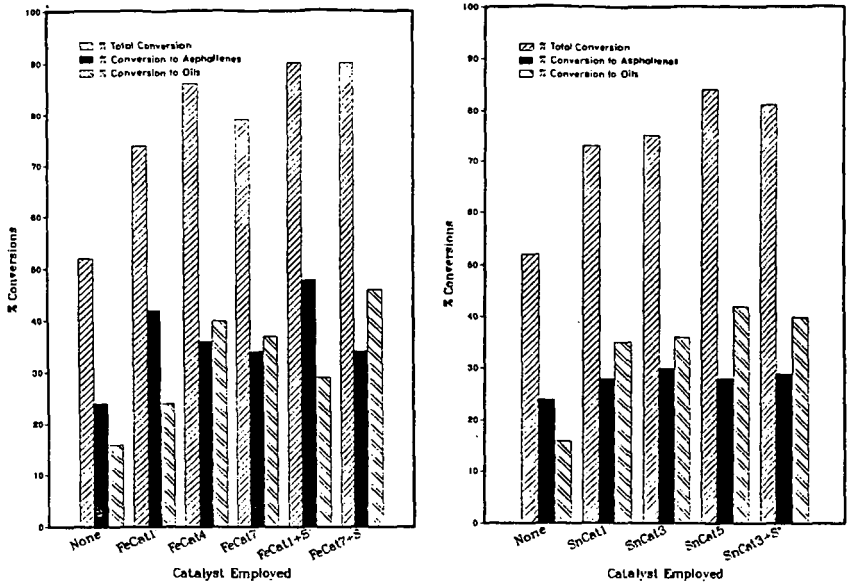


Figure 1. Activities of The Sulfate-Treated Iron and Tin Oxides for Liquefaction of Argonne Illinois No.6 Coal at 400°C, 1000 psig H₂, 1 hr run time

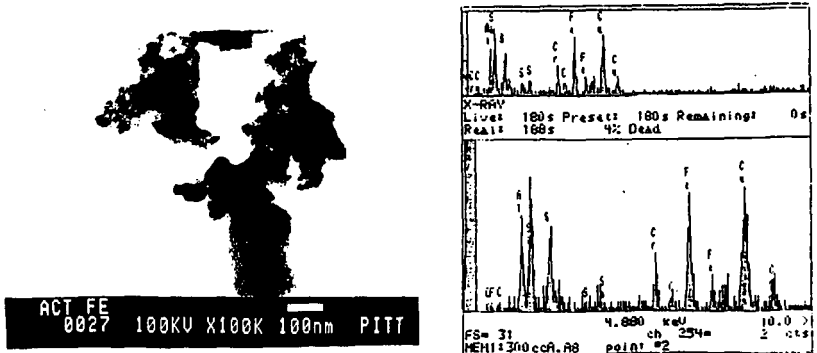


Figure 2. TEM-mode image of iron-containing particles on activated carbon and EDX Spectrum of Coal Liquefaction Residue using sulfated Iron Oxide Catalyst

References

1. Derbyshire, F. J., Catalysis in Coal Liquefaction: New Directions for Research, (IEA CR-08, London, U.K., IEA Coal Research, Jan. 1988).
2. Cugini, A. V., Lett, R. G., Energy and Fuels, (1989), Vol. 3, pp. 120-126
3. Weller, S., Pelipetz, M. G., Industrial and Engineering Chemistry, (1951), Vol. 43, No. 5, pp. 1243-1246
4. Derbyshire, F. J., Energy and Fuel, (1989), Vol. 3, No. 3, pp. 273-277.
5. Garg, D., Givens, E., Ind. Eng. Chem. Proc. Des. Dev., (1982), Vol. 21, pp. 113-117
6. Suzuki, T., Yamada, H., Sears, P., Watanabe, Y., Energy and Fuels, (1989), Vol. 3, pp. 707-713
7. Cugini, A. V., Utz, B. R., Fromell, E. A., Preprints, Div. of Fuel Chemistry, Am. Chem. Soc., Sept. 1989
8. Herrick, D. E., Ph.D. Thesis, University of Pittsburgh, 1990
9. Marriadassou, D., G., Charcosset, H., Andres, M., Chiche, P., Fuel, (1983), Vol. 62, pp. 69-72
10. Mukharjee, D. K., Mitra, J. R., Fuel, (1984), Vol. 63, pp. 722-723
11. Olah, G. A., Prakash, G. K. S., Sommer, J., Superacids, (New York: John Wiley and Sons, 1985), pp. 15-42.
12. Tanabe, K. in Heterogeneous Catalysis, (Texas A & M Univ., College Station, Texas, 1984), pp. 71-94.
13. Nakatani, Y., Sakai, M., Matsuoka, M., J. of Appl. Physics, Vol. 21, (1982), pp. L758
14. Tanabe, K., Yamaguchi, T., Hattori, H., Sanada, Y., Yokoyama, S., Fuel Processing Technology, (1984), Vol. 8, pp. 117-122
15. Tanabe, K., Yamaguchi, T., Hattori, H., Matsuhashi, H., Kimura, A., Fuel Processing Technology, (1986), Vol. 14, pp. 247-260
16. Kotanigawa, T., Yokoyama, S., Mitsuyoshi, Y., Maekawa, Y., Fuel, Vol. 68, (1989), pp. 531-533
17. Besson, M., Bacaud, R., Charcosset, H., Varloud, J., Fuel Processing Technology, (1986), Vol. 14, pp. 213-220
18. Besson, M., Bacaud, R., Charcosset, H., Sharma, B. K., Fuel, (1989), Vol. 69, pp. 213-220
19. Montano, P.A., Bommanavar, A. S., Shah, V., Fuel, (1981), Vol. 60, P. 703

PYRIDINE SORPTION BY PYRIDINE-EXTRACT
OF ILLINOIS NO. 6 COAL

Thomas K. Green and James E. Ball
Department of Chemistry
Center for Coal Science
Western Kentucky University
Bowling Green, KY 42101

KEYWORDS: Coal swelling, Extracts, Pyridine

INTRODUCTION

The principal goal of this research is to develop an understanding of the thermodynamics of the swelling of coals in various solvents. The approach is unique in the sense that the uncrosslinked portion of the coal is being swollen, as opposed to the crosslinked portion. This approach avoids complications due to the crosslinked nature of coals, and allows the experimental data to be interpreted in terms of modern theories developed for polymer solutions.¹

The uncrosslinked portion of the coal is obtained by pyridine-extraction of the coal. The extract is then swollen with the solvent at several relative pressures until equilibrium is established. In principle, free energies, enthalpies, and entropies of swelling can be determined from such an approach.

We are currently working with the pyridine-extract of an Argonne premium Illinois No. 6 coal. This coal is about 27% (wt) Soxhlet extractable in pyridine. The carbon, hydrogen and nitrogen contents of the extract are very similar to those of the original coal. The extract was exposed to pyridine at several relative pressures and the equilibrium weight of pyridine was measured. Studies were conducted at both 50°C and 70°C. We also studied the O-methylated extract under the same conditions.

EXPERIMENTAL

Sample preparation. Argonne Premium Illinois No. 6 coal was obtained from Argonne National Laboratory in ampoules of five grams of -100 mesh coal. The coal was first dried under vacuum at 105°C to constant weight and then analyzed for carbon, hydrogen, and nitrogen. Analysis found: C, 65.57; H, 4.66; N, 1.24 (duplicate).

Approximately 4.5 g of the sample was Soxhlet-extracted with dry pyridine under argon for several days until the siphon liquid was clear. The pyridine solution was then filtered through a 0.4 μ m nylon membrane filter to insure removal of particulates and colloidal material. The filter did not plug. Most of the pyridine was removed by rotovaporization under reduced pressure at 70-80°C. Approximately 200 mL of a methanol/water (80/20 vol.) mixture and 2 mL of conc. HCl were added to the flask and the mixture was stirred under nitrogen for two days. The solid extract was then filtered and dried under vacuum at 105°C for 24 hours. The extractability was 27.2% (wt.). This value agrees well with that found by Buchanan et al.² Analysis found: C, 78.32; H, 5.62; N, 1.65 (duplicate).

The pyridine-insoluble residue obtained from the extraction was first dried under vacuum to remove most of the pyridine, treated with the methanol/water/HCl mixture, and then dried under vacuum. Analysis found: C, 60.47; H, 4.39; N, 1.30 (duplicate).

The extract was O-methylated according to the procedure of Liotta.³ FT-IR analysis and carbon and hydrogen analysis confirmed that reaction had occurred. Analysis found: C, 76.7; H, 6.04; N, 1.24.

Sorption Experiments. Sorption experiments using pyridine as solvent were carried out using a quartz spring balance shown in Figure 1. The balance consists of a quartz spring, a large 5 liter flask, vacuum inlet system, and MKS pressure transducer (0-1000 torr, 0.5% accuracy). The entire balance chamber, including transducer, is housed in a Precision Scientific circulating (forced air) drying oven, which is maintained at a constant temperature by a I²R thermowatch temperature regulator which activates a light bulb.

The sample is suspended from the quartz spring and, as the sample sorbs solvent, the spring extends until equilibrium is reached. The extension of the spring is measured through a window on the door of the oven using a sensitive Eberbach cathetometer (travelling telescope). The spring is calibrated at the appropriate temperature using standard weights before the experiment is conducted. The experiment thus allows determination of the mass of solvent sorbed by the sample at a given partial pressure and temperature. The purpose of the 5 liter flask to minimize pressure changes caused by sorption of solvent by the sample. Quartz springs of the type used here have a linear-extension versus suspended-weight relationship and exhibit no hysteresis within the range of weights for which the spring is designed.

For the particular spring used in these experiments, the calibration factor was determined to be 0.48 mm/mg. The uncertainty of the cathetometer is ± 0.1 mm. Since two measurements must be made to obtain the weight of solvent, the uncertainty in the solvent weight is ± 0.2 mm \times 1 mg/0.48 mm = ± 0.4 mg. In a typical experiment, 50 mg of extract was used, so the uncertainty per gram of extract is ± 0.4 mg/0.050 g = ± 8 mg/g extract.

The experimental procedure was as follows. Approximately 50 mg of extract was placed in the quartz bucket and weighed on an electronic balance. The bucket and sample were then suspended on the spring. The hangdown tube was replaced and the system was evacuated to less than 0.1 torr and brought to the appropriate temperature. The system was allowed to evacuate overnight. Purified pyridine was placed in the round bottom flask shown in Figure 1 and frozen with dry ice/isopropanol. Stopcock B was closed, and stopcock C was opened to evacuate air from the flask. Then stopcock C was closed, and the pyridine was thawed and refrozen. Stopcock C was again reopened for evacuation. This procedure insures removal of last traces of air. Stopcock A was closed and stopcocks B and C were then opened until the appropriate pressure of pyridine was reached. After equilibrium was achieved, the pressure of pyridine was again raised. This procedure was repeated until the entire pressure range was covered.

RESULTS

Characterization of Pyridine Extract. Residual pyridine was removed from the pyridine-extract of the Argonne Illinois No. 6 coal by stirring with a methanol/water/HCl mixture for two days. Elemental analyses of the pyridine-extract revealed 1.65% N compared to 1.47% N (daf) in the original coal. The possibility exists that a small amount of pyridine remains bound to the extract. If one assumes that the additional N content of 0.18% is attributed to residual pyridine, then 10 mg pyridine/g extract was not removed from the extract by the methanol/water/HCl washing. FT-IR analysis failed to detect any residual pyridine, however.

The O-methylated extract was analyzed for carbon and hydrogen to establish the number of methyl groups added. The H/C ratio of the original extract is 0.86 and

the ratio of the O-methylated extract is 0.94. This increase in H/C ratio corresponds to the addition of 7.5 methyl groups per 100 carbon atoms of original extract. Liotta determined that there were approximately 5 acidic hydroxyl groups in an Illinois No. 6 coal,³ which is considerably lower than that determined here. However, our value is for the extract, not the whole coal, and it does not seem unreasonable. The O-methylated extract exhibited a reduced hydroxyl group absorption compared to the original extract, consistent with the conversion of phenolic hydroxyl groups to methyl ethers. In addition, a significant absorption at 1700 cm^{-1} appears in the spectrum of the O-methylated extract, consistent with the conversion of carboxylic acids to methyl esters.

Sorption Experiments. The pyridine-extract and O-methylated extract of the Argonne Illinois No. 6 coal were exposed to pyridine at various vapor pressures at 50°C and 70°C . Several incremental sorption experiments were conducted in that, once equilibrium was attained at a particular pressure, the pressure was raised, and the system was again allowed to attain equilibrium. Typical sorption curves for the extract and O-methylated extracts are shown in Figures 2 and 3, respectively. Note that a wide range of pressures was covered, ranging from 0.20 to 0.99. For the extract, several hours are required to reach equilibrium at each pressure and, in general, equilibrium was achieved more rapidly at the higher pressures. Equilibrium was achieved more rapidly for the O-methylated extract in comparison, particularly at the lower pressures.

The equilibrium amounts of pyridine determined from each sorption experiment are plotted against relative pressure of pyridine in Figure 4. Note that there is a good straight-line correlation between the sorption values and pressure for each extract and each temperature. The curves drawn are least-squares fits. The slope of the curve decreases upon O-methylation, i.e. the O-methylated extract sorbs less pyridine at equivalent relative pressures. Both extracts sorb less pyridine at the higher temperature.

DISCUSSION

The results in Figure 4 demonstrate that sorption of pyridine by the extract of the Illinois No. 6 coal obeys Henry's Law, i.e. the solubility of pyridine in the extract increases linearly with pressure. However, the curves do not pass through the origin. This result is similar to those of Michaels *et al.*, who observed that the solubilities of several gases in polyethylene terephthalate obeyed Henry's law.⁴ For two of the gases, carbon dioxide and ethane, the sorption isotherms were curved at low pressures but linear at higher pressures. They interpreted their results by proposing that sorption took place by two concurrent mechanisms at the lower pressures; ordinary dissolution and "hole-filling". At higher pressures, the holes or microvoids were saturated with only dissolution occurring. The intercept was interpreted as the total amount of sorption due to filling of the microvoids. Thus, a quantitative separation of the two processes was possible.

Following the work of Michaels *et al.*, we suggest that the intercepts observed in Figure 4 represent the total amount of pyridine that fills holes in the extracts. Using a density of 0.98 g/mL for pyridine, the total microvoid volume occupied by pyridine is determined to be 0.079 mL per g of extract (average of two values). Using a density of 1.3 g/mL for the extract (determined with helium), this corresponds to 9% microvoid volume for the extract. The same calculation for the O-methylated extract yields a value of 7% microvoid volume. Although caution is warranted at this time, we feel the magnitude of these values is reasonable.

Finally, we have corrected the sorption curves shown in Figure 4 for hole-filling according to the above model. The results are shown in Figure 5. These curves represent dissolution of pyridine into the extracts if our interpretation is

correct. We can calculate the differential heats of dilution for both the extract and the O-methylated extract from the data using Equation 1. The differential heat of dilution is defined as the heat change when one mole of pyridine is added to an infinite amount of the mixed phase at the specified concentration, and is given by

$$\Delta H_{d11} = \frac{-RT^2 d(\ln p/p_0)}{dT} \quad (1)$$

For the case in which solubility follows Henry's law, the heat of dilution is constant as a function of concentration, as long as the curves have the same intercept. Using a average temperature of 333 K, we calculate a ΔH_{d11} of -2.3 kcal/mole for the extract-pyridine system and a value of -4.5 kcal/mole for the O-methylated extract-pyridine system.

We feel the sign and magnitude of ΔH_{d11} calculated for the extract-pyridine system is reasonable, since pyridine is expected to hydrogen bond to phenolic groups in the extract, a process which is expected to be exothermic. Although the strength of hydrogen bonds between pyridine and phenols are typically on the order of 7 kcal/mole,³ it must be considered that coal-coal hydrogen bonds probably have to be broken in the extract in order to form a pyridine-coal hydrogen bond. (It is obvious in the IR spectrum of the extract that the hydroxyl groups in the extract must be hydrogen bonded). This process obviously costs energy, so the magnitude of ΔH_{d11} for this system is not unreasonable.

The more negative ΔH_{d11} for the O-methylated extract is surprising, particularly since hydrogen bonding is expected to be absent in this system. We currently have no explanation for this result. We simply suggest that perhaps there is a small population of sites in the O-methylated extract which interact strongly with pyridine. The nature of these sites is unknown, but they may be hydroxyl groups that were left unreacted by O-methylation. Clearly, more studies need to be done before conclusions can be drawn.

Finally, we note that the curves in Figure 4 indicate that there should be only limited swelling of the extracts at a relative pressure of 1.0. However, we have noted that both extracts can be substantially redissolved in liquid pyridine ($p/p_0=1.0$). Thus, it seems that the curves must rise very steeply as a relative pressure of 1.0 is approached. The data shown in Figure 4, however, do not support this idea. We presently have no explanation for this result.

CONCLUSIONS

Equilibrium sorption of pyridine by the pyridine-extract and the O-methylated extract of the Illinois No. 6 coal increases linearly with pressure. We tentatively interpret the intercept as the total amount of pyridine that fills microvoids in the extract. Equilibrium sorption of pyridine decreases with increasing temperature at equivalent relative pressures for both extracts, consistent with exothermic processes. We are currently conducting experiments on the whole coal to see if it might behave similarly. The results will be presented in the talk.

ACKNOWLEDGEMENTS

We gratefully acknowledge the Department of Energy, Grant No. DE-FG22-88PC88924, and the Research Corporation for support of this work.

REFERENCES

1. Treloar, L.R.G., "The Physics of Rubber Elasticity," Clarendon Press, Oxford, 1975, 128-129.
2. Buchanan, D.H.; Warfel, L.C.; Bailey, S.; Lucas, D., Energy Fuels, 1988, 2(1), 32-36.
3. Liotta, R.; Rose, K.; Hippo, E., J. Org. Chem., 1981, 50 277-283.
4. Michaels, A.S.; Vieth, W.V.; Barrie, J.A., J. Appl. Phys., 1963, 34, 1-12.
5. Arnett, E.M.; Joris, L.; Mitchell, Murty, T.S.S.R.; Gorric, T.M.; Schleyer, P.v.R., J. Am. Chem. Soc., 1970, 92, 2365.

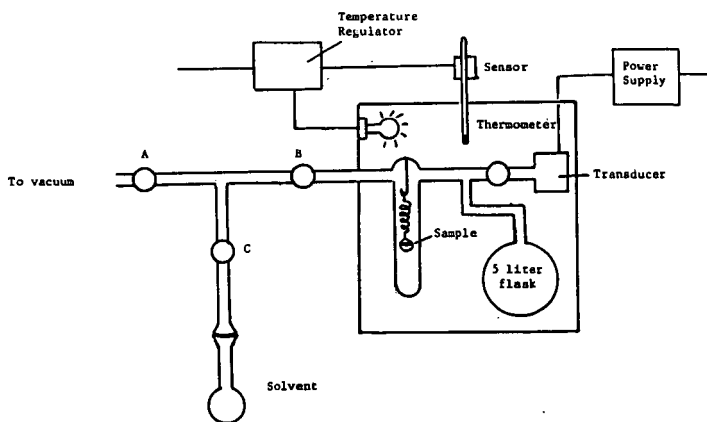


Figure 1. Sorption Apparatus

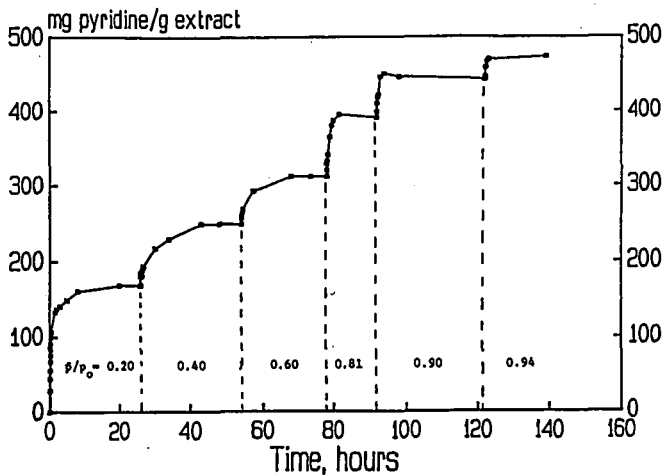


Figure 2. Sorption of Pyridine by Pyridine-extract of Illinois No. 6 Coal at 50°C.

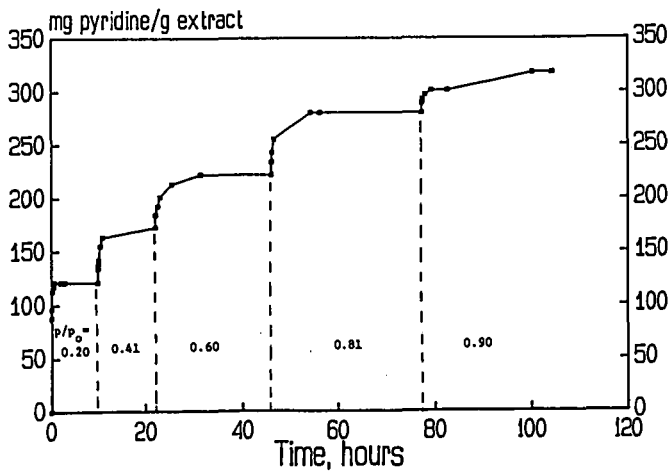


Figure 3. Sorption of Pyridine by O-methylated Pyridine-extract of Illinois No. 6 Coal at 50°C.

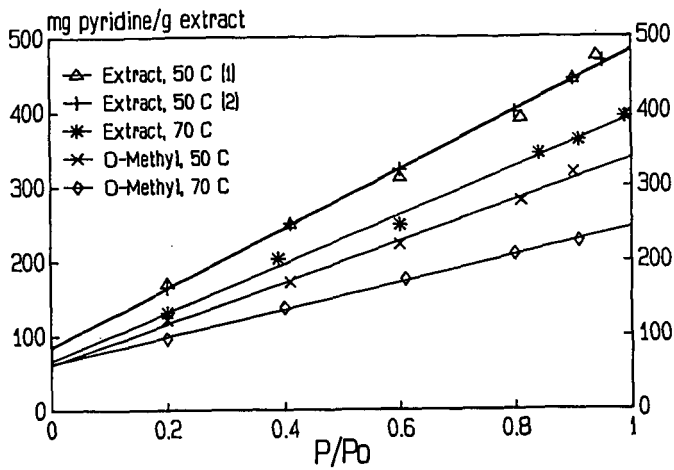


Figure 4. Sorption Isotherms of Pyridine-extracts of Illinois No. 6 Coal.

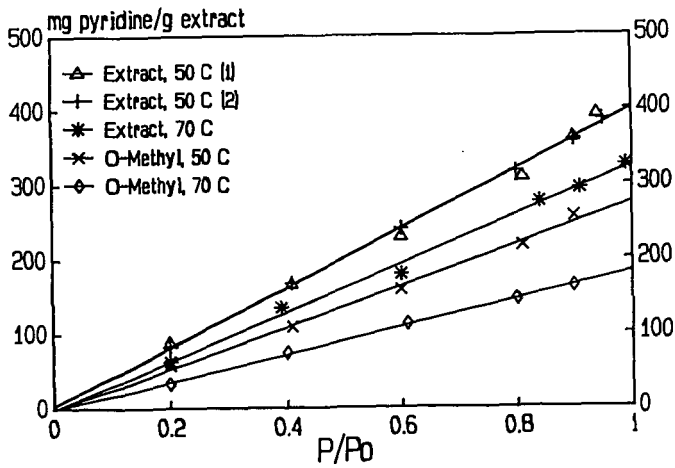


Figure 5. Corrected Sorption Isotherms of Pyridine-extracts of Illinois No. 6 Coal.

KINETICS OF VOLATILE PRODUCT EVOLUTION FROM THE ARGONNE PREMIUM COALS

Michael A. Serio, Peter R. Solomon, Sylvie Charpenay, Zhen-Zhong Yu,
and Rosemary Bassilakis

Advanced Fuel Research, Inc., 87 Church Street, East Hartford, CT 06108

Keywords: Coal Pyrolysis, Kinetics, Argonne Premium Coals

ABSTRACT

This paper describes the development of a set of rank dependent kinetic parameters for the evolution of the major volatile species from pyrolysis of the eight Argonne Premium coals. Programmed pyrolysis experiments are done over a range of heating rates (3, 30, 50, 100 °C/min) in an instrument which combines Thermogravimetric Analysis (TG) with evolved product analysis using Fourier Transform Infrared Spectroscopy (FT-IR) (the Bomem TG/Plus). An analysis of the data on the temperature for the peak evolution rate (T_{max}) for tar, CH_4 , and CO_2 as a function of heating rate is used for obtaining a preliminary estimate of the mean kinetic parameters. The parameters are further refined by using the FG-DVC model for coal pyrolysis to best fit the complete evolution profiles at each of the four heating rates. A final test is done by use of the parameters to predict pyrolysis data obtained under high heating rate conditions. The kinetics are found to vary systematically with rank and are faster for lower rank coals. The variations with rank are most significant for high rank coals with greater than ~ 86% daf carbon (< 8% daf oxygen). These differences can be important in accurately predicting coal fluidity and ignition phenomena.

INTRODUCTION

This paper is a continuation of work reported previously, related to the measurement and modeling of the pyrolysis kinetics for the Argonne Premium coals (1-3). In the first paper (1), the results for pyrolysis of the Argonne Premium coals at 30 °C/min in the TG-FTIR and 3 °C/min in a Field Ionization Mass Spectrometer (FIMS) apparatus were reported. Comparisons were made of the T_{max} values for the evolution of major volatile products and the molecular weight distributions (MWD) of the tars from pyrolysis-FIMS experiments. In the next paper (2), the FG-DVC coal pyrolysis model was used to simultaneously fit the pyrolysis data from the 30 °C/min TG-FTIR experiments, the 3 °C/min (vacuum) FIMS experiments and the ~ 5000 K/s entrained flow reactor (EFR) experiments.

The third paper (3) was a preliminary evaluation of the rank dependence of the pyrolysis kinetic rates for tar, CH_4 , and weight loss for the Argonne coals based on TG-FTIR experiments at four different heating rates with all eight coals and from entrained flow reactor experiments in a Transparent Wall Reactor (TWR) with two of the coals (Zap lignite, Pittsburgh Seam bituminous) at ~ 5000 K/s. In the current paper, the rank dependent kinetic parameters have been further refined and developed for additional species (CO_2). For the Illinois coal, an extrapolation has been made to high heating rate conditions for the case of tar evolution.

EXPERIMENTAL

Coal Properties

The elemental and ultimate analysis data for the Argonne Premium coals are given in Refs. 4 and 5.

Reactor System

Pyrolysis experiments were done with the Argonne premium coals at heating rates of 3, 30, 50, and 100 °C/min up to 900 °C in a TGA with FT-IR analysis of evolved products (TG-FTIR). The TG-FTIR apparatus consists of a sample suspended from a balance in a gas stream within a furnace. As the sample is heated, the evolving tars and gases are carried out of the furnace directly into a 5 cm diameter gas cell (heated to 150 °C) for analysis by FT-IR. With this geometry under low heating rate conditions, the temperature of the sample is assumed to be the same as that of a thermocouple which is next to the sample. The TG-FTIR system used in the current work is the TG/Plus from Bomem, Inc.

The TG/Plus couples a Dupont 951 TGA with a Bomem Michelson 100 FT-IR spectrometer (6,7).

High heating (~ 20,000 K/s) pyrolysis rate measurements were previously made in a heated tube reactor (HTR) with an Illinois No. 6 coal, as described in Ref. 8. These experiments included in-situ FT-IR diagnostics for measurement of the coal particle temperature. A heat transfer model was developed which provided a good fit to the measured temperature profile (8,9). The predictions of the heat transfer model were subsequently input into the FG-DVC pyrolysis model.

RESULTS

The TG-FTIR results for the Pittsburgh Seam coal at three heating rates are given in Fig. 1. The dashed lines are the prediction of the FG-DVC model (9-11) while the experimental data are plotted as asterisks connected by solid lines. The left hand set of curves is for the cumulative weight loss from the balance. Superimposed on each of these plots is the time-temperature profile. Except for very low heating rates, the coal is heated first to 150°C for drying before heating at the designated rate to 900°C.

The agreement between the experimental and predicted weight predictions is quite good at each of the three heating rates. The predicted weight loss is the sum of the tar evolution and the major gases (CO, CO₂, H₂, H₂O, CH₄, paraffins, olefins) which are included in the FG-DVC model.

The middle set of curves in Fig. 1 is for the tar evolution while the right hand set is for CH₄ evolution. The prediction of tar evolution is based on the breaking of weak linkages between an assumed polymeric structure for coal followed by transport of the molecule out of the coal if it meets the volatility criteria (10). The position and shape of the main tar peak is predicted very well for the Pittsburgh Seam coal and for several other coals that have been tested. The early part of the tar evolution is not as well predicted. This part of the tar evolution arises primarily from "guest" molecules which are physically bound in the coal. We are working on a new version of the FG-DVC model which includes the guest molecules (11).

The evolution of CH₄, shown on the far right hand side of Fig. 1 is also well predicted. The CH₄ evolution is modeled using two sources which evolve in a manner such that the peaks are usually merged into a single peak (9,10).

Both the tar and CH₄ evolution profiles show a systematic shift with increasing heating rate. The change in the temperature for the maximum evolution rate (T_{max}) with temperature can be used in preliminary analysis to derive kinetic parameters (12,13). We have used this approach to obtain a preliminary estimate of the mean values of the distributed activation energy parameters. The parameters are further refined by using the FG-DVC model to best fit the complete evolution profiles at each of four heating rates.

Similar comparisons are made in Figs. 2-5 for other coals in the Argonne series. In this case, the data are shown for a single heating rate (30°C/min) but one additional species (CO₂). Again, good agreement is obtained for the actual weight loss and the predicted values from all four coals. In the case of the Utah Blind Canyon coal and the Zap lignite, the predicted curves have been horizontally displaced to match the weight loss after moisture evolution since the model predictions are all done on a dry basis.

The prediction of the tar evolution profile is also good except for the very early tar as discussed above for the Pittsburgh Seam coal. The methane evolution profile is very well predicted in each case. The CO₂ evolution profiles are not as well predicted as the evolution of hydrocarbon species. The CO₂ evolution is predicted based on three assumed sources (extra loose, loose, and tight) (9,10). At 30°C/min, the peaks are centered at approximately 16, 22, and 28 minutes, respectively. However, because the mineral sources are not included in the model, the quality of the fits is not the same as for hydrocarbon species where there are no mineral contributions.

DISCUSSION

The use of the TG-FTIR method over a range of heating rates has allowed the development of a set of rank dependent kinetic parameters for tar, CH₄, and CO₂ (and indirectly the weight loss). The

parameters for the tar evolution were obtained by adjusting the value of the pre-exponential and activation energy for the bridge breaking rate in the FG-DVC model in order to match the evolution profiles at the four heating rates. In general, these rates increase monotonically with decreasing rank (increasing oxygen content). For very low rank coals, the contribution of polymethylenes is sufficiently large that it partly obscures the tar evolution from bridge breaking. In this case, the TG-FTIR results from demineralized coals are used to obtain a more reliable estimate of the bridge breaking rate. The lower amount of crosslinking in the demineralized coals reduces the relative contribution of the polymethylene tar.

In the case of the CH_4 and the CO_2 , good results were obtained by adjusting only the pre-exponential factors. The values of the activation energies used were the same as those reported previously (10).

The importance of the rank dependence of the pyrolysis kinetics for tar and CH_4 evolution was evident in the modeling of coal fluidity behavior (14). When modeling fluidity, it was found that relatively small differences in the methane evolution rate (which is related in our model to the moderate temperature crosslinking which shuts down the fluidity) and the tar evolution rate (which is based on the bridge breaking rate as discussed above) have a large effect on the fluidity predictions. In Fig. 6 are shown comparisons of the measured fluidity with the predicted fluidity (based on the rank dependent rates) for five of the eight coals. With the possible exception of the Pocahontas coal, the agreement between the measured and predicted fluidity is quite good.

A good test of the validity of using the TG-FTIR method over a range of low heating rates to obtain kinetic parameters is the ability to use the kinetic parameters to extrapolate to high heating rate conditions. An example of this is shown in Fig. 7, where the parameters obtained for the Illinois No. 6 coal using the TG-FTIR method were used to simulate previously obtained high heating rate (~ 20,000 K/s) data for tar evolution (9). Again, the agreement between the theory and data is quite good.

Finally, a comparison can be made for results obtained for T_{max} for tar evolution at 3°C/min for the eight Argonne premium coals using the TG-FTIR method with results obtained by Burnham et al. (15) using a Rock-Eval experiment at 4°C/min. This comparison is shown in Fig. 8. The agreement between the two experiments is generally very good.

CONCLUSIONS

The conclusions of this work are as follows:

- The TG-FTIR method has been used to provide a set of rank dependent kinetic parameters for tar, CH_4 , CO_2 , and weight loss for the eight Argonne coals.
- These rank dependent kinetic parameters will be important in predicting fluidity and ignition behavior.
- The parameters obtained by this method extrapolate well to high heating rate conditions.
- Good agreement was found with low heating rate kinetic data obtained elsewhere with a different technique.

ACKNOWLEDGEMENTS

This work was supported under DOE Contract DE-AC21086MC23075. Richard Johnson is the Project Manager.

REFERENCES

1. Serio, M.A., Solomon, P.R., and Carangelo, R.M., ACS Div. of Fuel Chem. Preprints 33, (2), 295, (1988).
2. Serio, M.A., Solomon, P.R., Yu, Z.Z., Desphande, G.V., and Hamblen, D.G., ACS Div. of Fuel Chem. Preprints, 33, (3), 91, (1988).

3. Serio, M.A., Solomon, P.R., Yu, Z.Z., Bassilakis, R., ACS Div. of Fuel Chem. Preprints, **34**, (4), 1324, (1989).
4. Vorres, K.S., ACS Fuel Chem. Div. Preprints, **33**, (3), 1, (1988).
5. Vorres, K.S., Users Handbook for the Argonne Premium Coal Sample Program, Argonne National Lab., (September 1989).
6. Carangelo, R.M., Solomon, P.R., and D.G., Gerson, Fuel, **66**, 960, (1987).
7. Whelan, J.K., Solomon, P.R., Deshpande, G.V., and Carangelo, R.M., Energy & Fuels, **2**, 65, (1988).
8. Solomon, P.R., Serio, M.A., Carangelo, R.M., and Markham, J.R., Fuel, **65**, 182, (1986).
9. Serio, M.A., Hamblen, D.G., Markham, J.R., Solomon, P.R., Energy & Fuel, **1**, 138, (1987).
10. Solomon, P.R., Hamblen, D.G., Carangelo, R.M., Serio, M.A., and Deshpande, G.V., Energy & Fuel, **2**, 405, (1988).
11. Solomon, P.R., Serio, M.A., Hamblen, D.G., Yu, Z.Z., and Charpenay, S., ACS Div. of Fuel Chem. Preprints, **35**, (2), 479, (1990).
12. Jüntgen, H. and Van Heek, K.H., Fuel, **47**, 103 (1968) and "Progress Made in the Research of Bituminous Coal," paper given at the annual meeting of the DGMK, Salzburg, (1968), Translated by Belov and Associates, Denver, CO, APTIC-TR-0779 (1970).
13. Braun, R.L. and Burnham, A.K., Energy & Fuels, **1**, 153, (1987).
14. Solomon, P.R., Best, P.E., Yu, Z.Z., and Deshpande, G.V., ACS Div. of Fuel Chem. Preprints, **34**, (3), 895, (1989).
15. Burnham, A.K., Oh, M.S., Crawford, R.W., and Samoun, A.M., Energy & Fuel, **3**, 42, (1989).

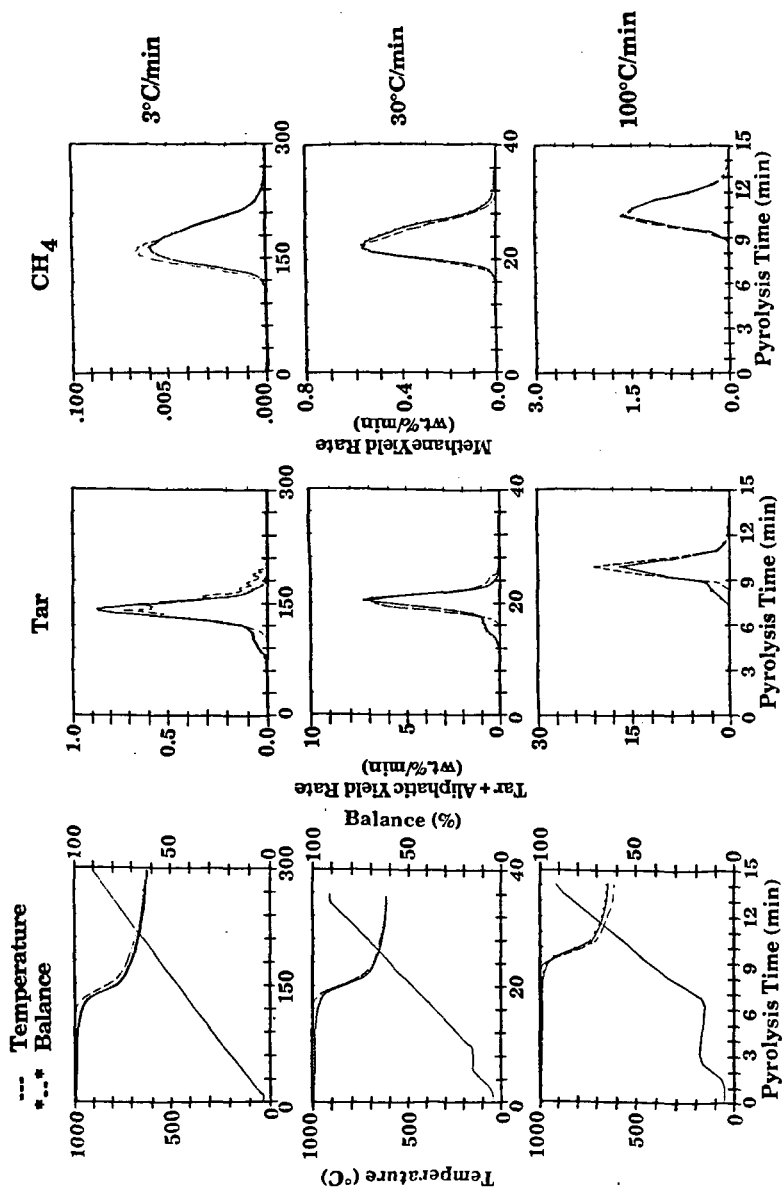


Figure 1. Kinetic Analysis at Three Heating Rates for Pittsburgh Seam Coal. Comparison of Theory (---) and Data (---).

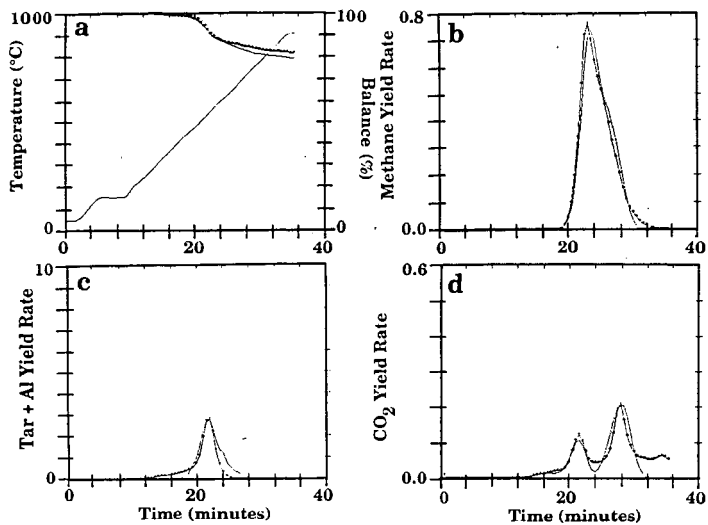


Figure 2. Kinetic Analysis at 30°C/min for Major Volatile Products. Comparison of Theory (—) and Data (***) for Pocahontas Coal.

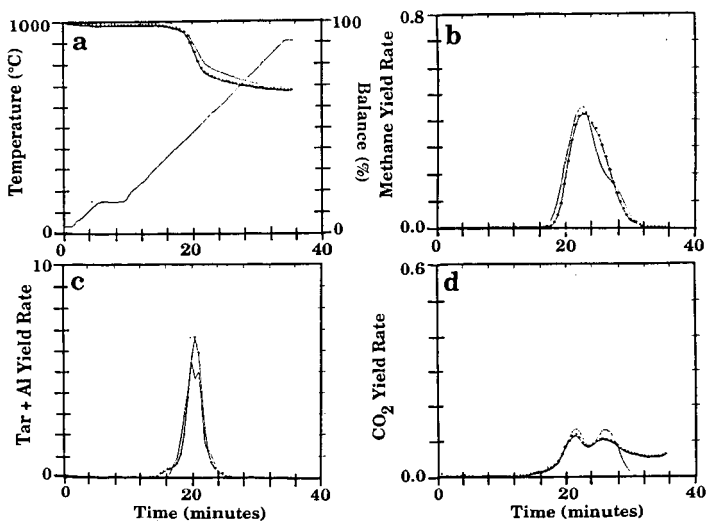


Figure 3. Kinetic Analysis at 30°C/min for Major Volatile Products. Comparison of Theory (—) and Data (***) for Lewis-Stockton Coal.

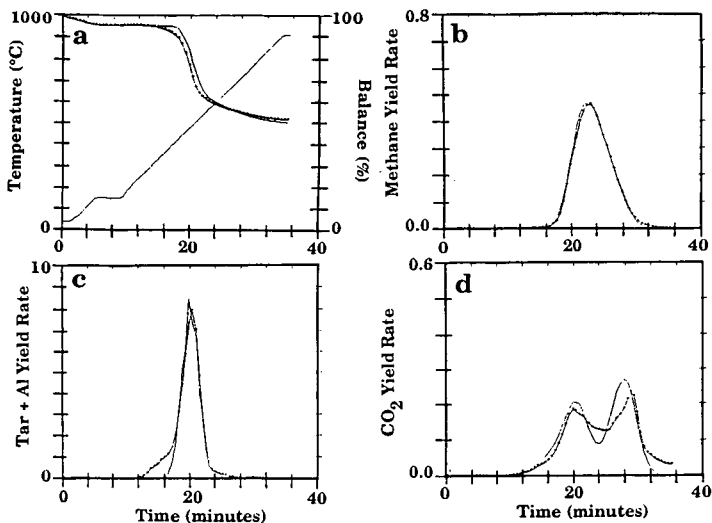


Figure 4. Kinetic Analysis at 30°C/min for Major Volatile Products. Comparison of Theory (—) and Data (*-*) for Utah Blind Canyon Coal.

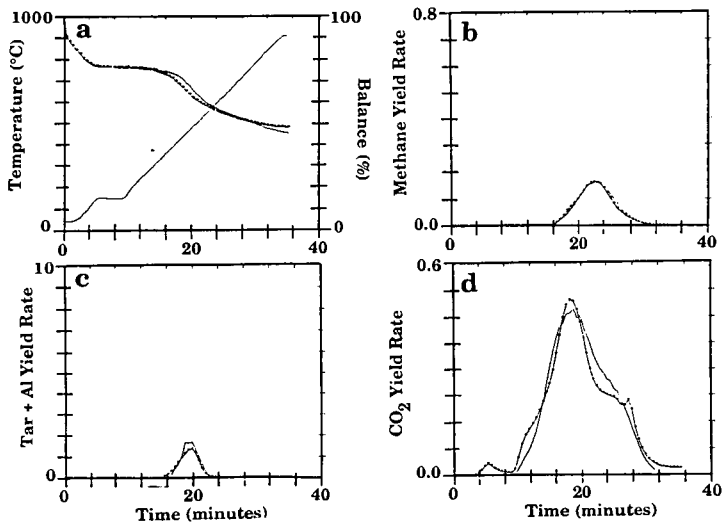


Figure 5. Kinetic Analysis at 30°C/min for Major Volatile Products. Comparison of Theory (—) and Data (*-*) for Zap Lignite

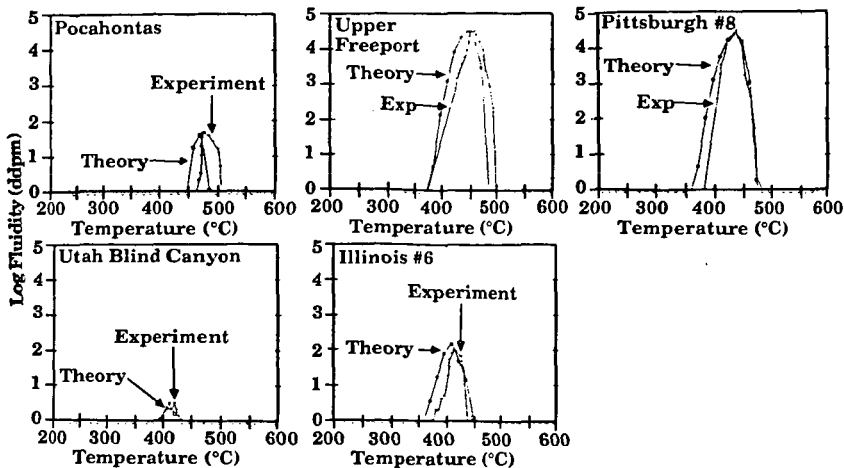


Figure 6. Comparison of Measured (**) and Predicted (o-o) Fluidity for Five Argonne Coals.

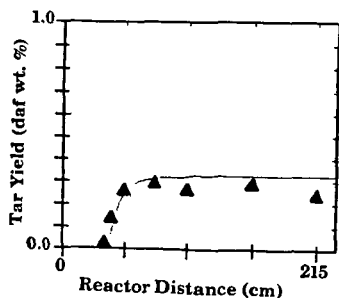


Figure 7. Pyrolysis Tar Yield Results for Illinois No. 6 Coal, 200 x 325 mesh, in the HTR at an Equilibrium Tube Temperature of 800°C. The Solid Lines are Predictions of the FG-DVC Model.

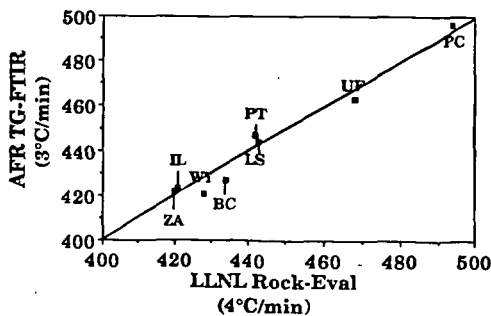


Figure 8. Comparison of AFR Data for T_{max} from TG-FTIR Analysis at 3°C/min with Rock-Eval Data from LLNL at 4°C/min.

A COMPARATIVE STUDY OF 8 US COALS BY SEVERAL DIFFERENT PYROLYSIS MASS SPECTROMETRY TECHNIQUES

Huaying Huai, Robert Lo, Yongseung Yun and Henk L.C. Meuzelaar
Center for Micro Analysis and Reaction Chemistry
EMRL 214 Building 61, University of Utah, Salt lake City, UT 84112

KEYWORDS: pyrolysis mass spectrometry, coal structure

ABSTRACT

Eight US coals of different rank and/or composition, obtained through the Argonne National Laboratory Premium Coal Sample Program, were analyzed by means of several different pyrolysis-MS (Py-MS) techniques, namely: direct Curie-Point Py-MS, Curie-point Py-GC/MS (including GC/EIMS, GC/CIMS and "short column" GC/CIMS), and vacuum thermogravimetry/MS (TG/MS). The data obtained were compared to Pyrolysis-Field Ionization MS (Py-FIMS) data.

The results show a very good agreement between all techniques used in spite of the marked differences in pyrolysis techniques (Curie-point, furnace, direct probe), "soft" ionization methods (low voltage EI, CI, FI) and mass spectrometer types (quadrupole, ion trap, magnetic sector) used. As might be expected, the most pronounced variations between techniques appear to be due to mass dependent differences in ion transmissivity and detector response, with the type of soft ionization method taking second place and the type of pyrolysis technique showing least effect on the results. Whereas Py-FIMS provides the most complete and detailed overview of the coal pyrolysis tars, Curie-point Py-MS and TG/MS methods provide more reliable information on relatively light gaseous products, and Curie-point Py-GC/MS shows the detail composition of the 2/3 of the total pyrolysis tars.

INTRODUCTION

The extremely complex nature of coal samples necessitates application of a wide range of sophisticated as well as conventional analytical techniques.

Pyrolysis mass spectrometry (Py-MS) is a relatively novel, advanced technique used for studying coals [1-5]. From an instrumental perspective, different Py-MS systems can be distinguished by: (1) pyrolysis technique, such as Curie-point pyrolysis, furnace pyrolysis and direct probe; (2) ionization method, such as electron ionization (EI), low voltage electron ionization (LVEI), Chemical ionization (CI), field ionization (FI), plasma desorption (PD), and fast atom bombardment (FAB); and (3) mass spectrometer type, such as quadrupole, ion trap, electric sector, magnetic sector, time-of-flight, and Fourier transform ion cyclotron resonance.

In this paper, several different Py-MS techniques, namely: direct Curie-point Py-MS, Curie-point Py-GC/MS (including GC/EIMS, GC/CIMS, "short column" GC/CIMS), and vacuum thermogravimetry/MS (TG/MS) were used for studying the 8 US coals from the Argonne National Laboratory Premium Coal Sample Program (ANL-PCSP). The results of a comparison between these methods as well as Py-FIMS will be discussed.

EXPERIMENTAL

Sample Collection and Preparation for Py-MS and Py-GC/MS

All 8 ANL-PSCP coals were obtained as 5 g, -100 mesh aliquots in dark tinted glass ampules closed under argon. The closed ampules were stored at -30 C until used. A 5-10 mg coal sample was suspended in 1-2 ml of Spectrograde methanol (5 mg/ml) and carefully hand-ground to a fine, uniform suspension. Then, a 5 μ l drop of the coal suspension was coated on the pyrolysis wire and air-dried. Next, the coated wire was inserted into a borosilicate glass reaction tube. Details of the sample preparation technique have been described by Meuzelaar et al. [1,6].

Curie-point Py-MS

Curie-point Py-MS was performed with an Extranuclear 5000-1 quadrupole Py-MS system as described previously [3]. The Py-MS conditions are listed in Table 1.

Curie-point Py-GC/MS

The Curie-point pyrolysis reactor [7] was controlled by a Fischer Labortechnik, 1.1 MHz, 1.5 kW high frequency power supply. A HP 5890a gas chromatograph using both regular (15 m) and short (4 m) fused silica capillary GC columns, and coupled directly to a Finnigan MAT 700 ITD mass spectrometer operating in EI or CI (isobutane) mode was used. Experimental conditions are shown in Table 1.

Vacuum Thermogravimetry/MS

Experiments were conducted on a Mettler TA1 thermoanalyzer coupled directly to a Finnigan MAT 3200 quadrupole MS system [5]. Table 1 shows details of the experimental conditions.

Py-FIMS

A Finnigan MAT 731 double-focussing magnetic sector mass spectrometer, a combined EI/FI/FD/FAB ion source and an AMD Intetra direct probe introduction system [8] was used for this experiment. Experimental conditions are given in Table 1.

RESULTS AND DISCUSSION

Figure 1 shows the mass spectra of three coals, Beulah Zap (lignite), Pittsburgh #8 (hvb) and Pocahontas #3 (lvb), obtained by Curie-point Py-MS at ambient inlet temperatures.

The spectra reflect the well-known fact that the pyrolysis products are coal rank dependent. The most prominent products from lignite (Beulah Zap) are oxygen-containing compounds, including (alkyl) phenols, (alkyl) dihydroxybenzenes and (alkyl) methoxyphenols. With increasing rank, the relative abundance of these oxygen-containing compounds decreases. The (alkyl) dihydroxybenzenes and (alkyl) methoxyphenols have nearly disappeared in the Pittsburgh #8 spectrum whereas (alkyl) naphthalene abundances have markedly increased. The most prominent pyrolysis products from Pocahontas #3 coal are aromatic and aliphatic hydrocarbons whereas oxygen-containing compounds are hardly detectable.

All other five Py-MS techniques show a similar rank dependence. With increasing rank aliphatic and aromatic oxygen-containing compounds decrease while aliphatic and aromatic hydrocarbon intensities increase. Rank effects on pyrolysis patterns observed by Curie-point Py-GC/MS, Py-FIMS and TG/MS have been discussed in more detail elsewhere [5,9].

Effect of Pyrolysis Method

Figures 1b, 2 and 3 illustrate the Py-MS patterns of Pittsburgh #8 coal as obtained by Curie-point, furnace and direct probe pyrolysis, respectively. As listed in Table 1, the detailed experimental conditions are quite different from one another, e.g., with regard to sample amount (25 μ g to 5 mg) and heating rate (1,000 C/sec to 25 C/min). However, as seen from Figures 1b, 2 and 3, the three techniques produce rather similar mass spectral patterns in the overlapping mass ranges, viz m/z 50-200. This may imply that the pyrolysis mechanisms are similar under the experimental conditions used.

Effect of Ionization Method

As expected, regular (70 eV) voltage electron ionization methods tend to break molecular ions into smaller fragment ions. Figure 4 shows that the dominant peaks are found at odd mass numbers in the low mass range. The spectra in Figures 1 and 2, however were produced by low voltage EI (12 eV and 14 eV, respectively). Consequently, molecular ions, seen primarily at even mass numbers because of the relatively low fragmentation of compounds as well as a low abundance of nitrogen compounds, dominate. However, as expected the CI spectra in Figures 5 and 6 are dominated by odd mass numbers due to the fact that most molecular ions are protonated $[M+H]^+$ forms. As shown in Figure 3, the FI technique produces largely even numbered molecular ions.

Variations between Methods

Notwithstanding the apparent similarities between the different techniques, as demonstrated in Figures 1-6, there are several other sources of variance that have not yet been discussed.

Except for the differences in pyrolysis techniques and type of quadrupole mass spectrometer used, distances between pyrolysis zone and ion source as well as transfer zone and ion source temperatures are comparable in Curie-point Py-MS and TG/MS techniques. Since, as shown above, differences in pyrolysis techniques appear to have minimal effect on pyrolysis mechanisms, the results from both techniques are quite similar (Figures 1 and 2).

Figure 3 shows the Py-FIMS results. Compared to Curie-point Py-MS and TG/MS, the distance between pyrolysis zone and ionization region is approx. 50% shorter. More importantly, ion source temperatures are higher and we are dealing with a different type of mass spectrometer (magnetic sector vs. quadrupole). Consequently, Py-FIMS detects far more high molecular weight components (Figure 3). Components below m/z 240 constitute only about 10-40% of the total signal intensity, depending on rank. Comparison of Figures 1 and 2, with Figure 3 indicates that Curie-point Py-MS and TG/MS detect only 10-40% of the total pyrolysis products, which agrees with previously published results [1]. The main reasons appear to be: (1) low transmissivity of quadrupole mass spectrometers in the higher mass ranges, and (2) unheated transfer zones and ion sources in the standard Curie-point Py-MS and TG/MS configurations causing condensation losses of large molecules (heating inlet system and ion source markedly increases signal intensities in the higher mass range [10] but also tends to lead to more rapid contamination of the ion source).

Figures 5 and 6 shows the effect of column length on Curie-point Py-GC/MS results. As expected, the use of short capillary GC columns at high linear carrier gas flow velocities enhances the detection of large molecules. The molecular weight averages (Table 2) shift some 15 to 60 mass units towards the high mass range. Compared to Py-FIMS, however, average Py-GC/CIMS molecular weight values are still considerably lower. Currently, efforts are underway to correct the molecular weight profiles obtained by short column Py-GC/CIMS for known differences in ion transmissivity between quadrupole, ion trap and magnetic sector MS systems.

CONCLUSIONS

1. The known rank dependence of coal pyrolysis products is readily detected by all six Py/MS techniques used.
2. Within the range covered by these six techniques, differences in heating rate and sample size do not have a strong effect on the distribution of coal pyrolysis products.
3. All three soft ionization methods used (CI, FI, low voltage EI) appear useful for studying molecular weight distributions.
4. Although the type of pyrolysis method used has little effect on the composition of the pyrolysis products, the choice of the product analytical method has a major influence.
5. Magnetic sector instruments, e.g., as used in FIMS appears to provide the most complete and detailed overview of the coal pyrolysis tars.
6. Py-GC/MS (EI and CI) is capable of providing detailed information on compounds in the molecular weight range up to m/z 400, representing about 2/3 of the total tar.
7. Finally, the information obtained by Curie-point Py-MS and TG/MS methods for high molecular tar products is strongly dependent on inlet and ion source temperatures.

ACKNOWLEDGEMENT

The authors wish to thank Drs. Hans-Rolf Schulten and Norbert Simmleit for performing the Py-FIMS analyses. This work was supported by DOE grant #UKRF-4-23576-90-10 (Consortium for Fossil Fuel Liquefaction Science).

REFERENCES

1. Harper, A.M., Meuzelaar, H.L.C., and Given, P.H., *Fuel*, 63, 793-802 (1984).
2. Marzec, A., *J. Anal. Pyrolysis*, 8, 241-254 (1985).
3. Metcalf, C.S., Windig, W., Hill, G.R., and Meuzelaar, *Int. J. Coal Geol.* 7, 245-268 (1987).
4. Tromp, P.J.J., Ph.D. Thesis, University of Amsterdam, (1987).
5. Yun, Y., Maswadeh, W., Meuzelaar, H.L.C., Simmleit, N., and Schulten, H.-R., *ACS Preprints, Div. Fuel Chem.*, 34(4), 1308-1316 (1989).
6. Meuzelaar, H.L.C., Haverkamp, J., and Hileman, F.D., "Curie-point Pyrolysis-Mass Spectrometry of Recent and Fossil Biomaterials; Compendium and Atlas", (Eds. H.L.C. Meuzelaar et al.), Elsevier, Amsterdam (1982).
7. Meuzelaar, H.L.C., McClennen, W.H., and Yun, Y., 35th ASMS Conf. on Mass Spec., All Topics, Denver, CO, May 24-29, 1142-1143 (1987).
8. Schulten, H.-R., Simmleit, N., Muller, R., *Anal. Chem.*, 59, 2903-2908 (1987).
9. Huai, H., Lo, R., and Meuzelaar, H.L.C., in preparation (1990).
10. Taghizadeh, K., Hardy, R.R., Davis, B.H., Meuzelaar, H.L.C., "Comparison of Low Voltage and Field Ionization Mass Spectra of Coal-derived Liquids from the Wilsonville Pilot Plant", submitted to *Fuels Processing Technology* (1990).

Table 1. Experimental Conditions

	Py-MS	TG/MS	Py-GC/MS			FIMS
			15m EI	15m CI	4m CI	
Sample Size (g)	2.5×10^{-3}	5.0×10^{-3}	2.5×10^{-3}	2.5×10^{-3}	2.5×10^{-3}	1.0×10^{-4}
Pyrolysis Method	Curie-point	Furnace	Curie-point	Curie-point	Curie-point	direct probe
Final Temp. (C)	610	700	610	610	610	750
Heating Rate (K/sec)	1×10^2	4×10^{-1}	1×10^2	1×10^2	1×10^2	1×10^0
Inlet Temp. (C)	≈ 100	≈ 100	290	290	290	≈ 200
Pressure in Pyrolysis Zone	high vacuum ($<10^{-4}$ torr)	high vacuum ($<10^{-4}$ torr)	30 p.s.i. (abs)	30 p.s.i. (abs)	25 p.s.i. (abs)	high vacuum ($\approx 10^{-3}$ torr)
Distance (from Pyrolysis Zone to Ion Source)	5 cm	5 cm	15 m	15 m	4 m	2 cm
MS Type	quadrupole	quadrupole	Ion Trap	Ion Trap	Ion Trap	magnetic sector
Ionization Method	EI (12 eV)	EI (14 eV)	EI (70 eV)	CI (isobutane)	CI (isobutane)	FI
Ion Source Temp (C)	≈ 100	≈ 100	230	230	230	200
Mass Range Scanned	20-240	33-200	50-450	90-500	100-600	50-900

Table 2. Molecular Weight Averages (\bar{M}_n)
Obtained by Different Techniques

Coal	Curie-point Py-GC/MS		FIMS
	15 m CI	4 m CI	
Beulah Zap	172	185	792
Wyodak-Anderson	184	203	338
Illinois #6	222	270	367
Blind Canyon	226	269	366
Pittsburgh #8	222	264	324
Lewiston-Stockton	218	263	327
Upper Freeport	223	277	386
Pocahontas #3	195	251	359

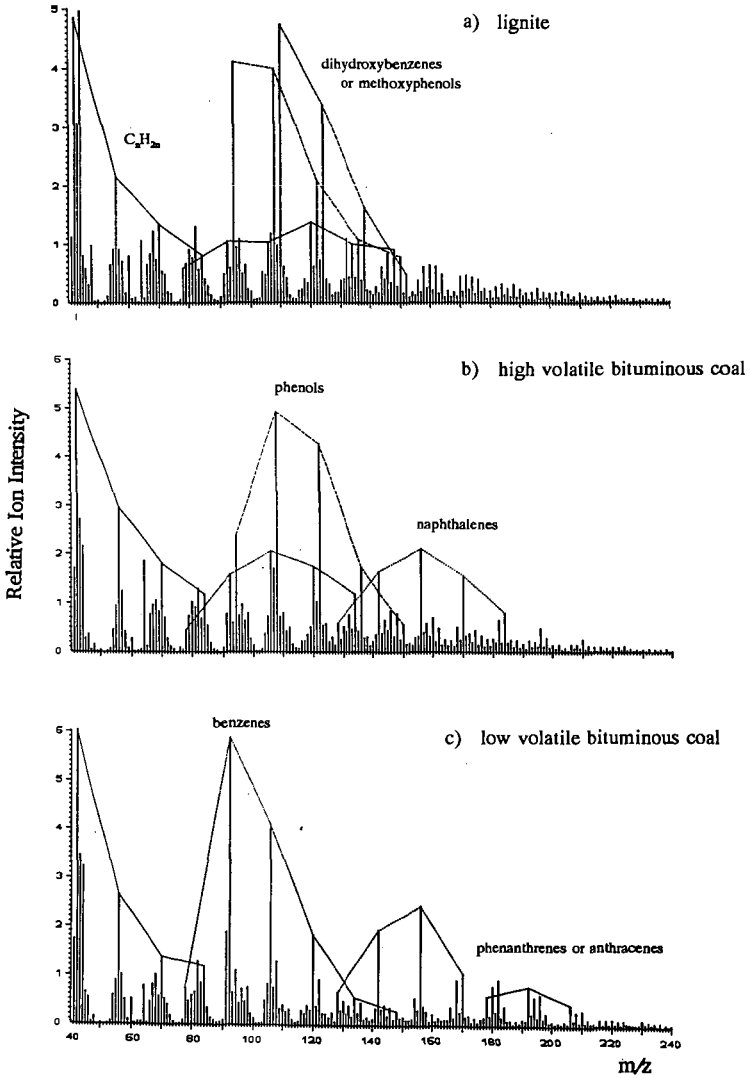


Figure 1. Curie-point pyrolysis low voltage EIMS spectra of a) Beulah Zap lignite, b) Pittsburgh #8, c) Pocahontas #3 coals.

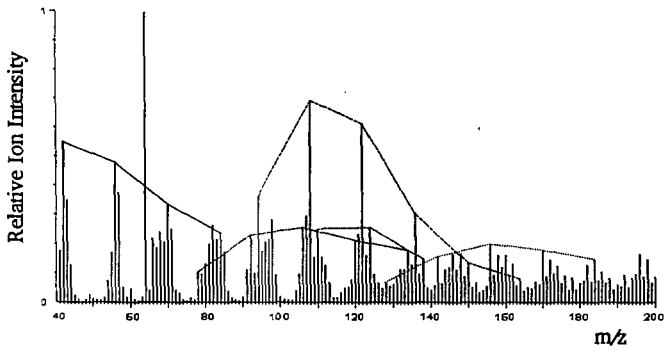


Figure 2. Mass spectrum of Pittsburgh #8 coal by TG/MS.

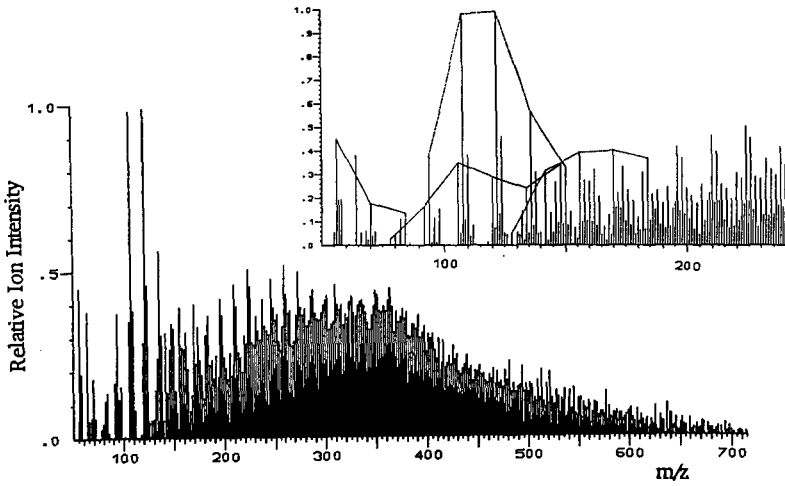


Figure 3. Mass spectrum of Pittsburgh #8 coal by Py-FIMS.

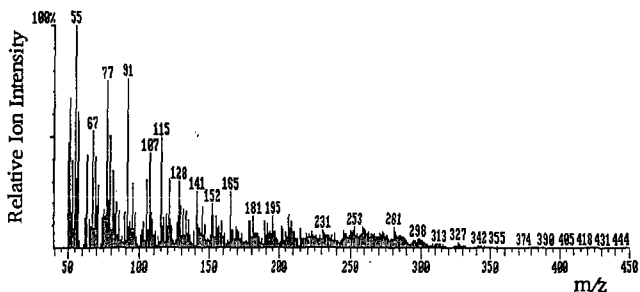


Figure 4. 70 Mass spectrum of Pittsburgh #8 coal obtained by Curie-point Py-GC/EIMS (70 eV).

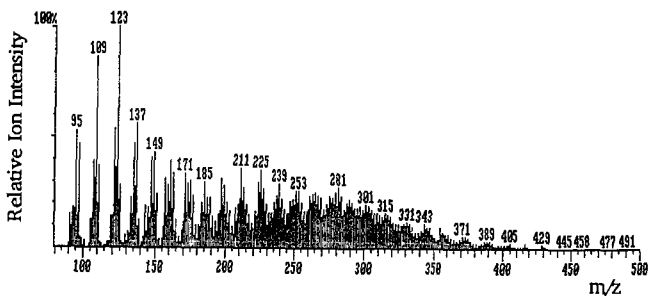


Figure 5. As Figure 4, obtained by Curie-point Py-GC/CIMS.

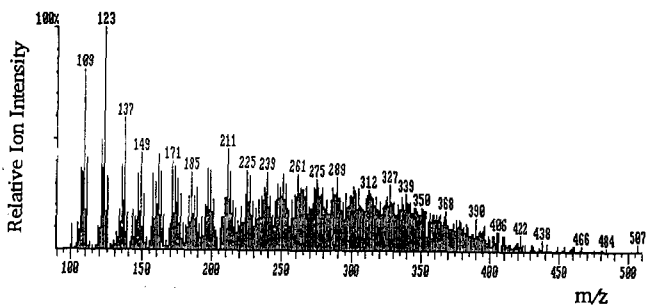


Figure 6. As Figure 4, but obtained by "short column" by Curie-point Py-GC/CIMS.

Ronald R. Martin, Jinjiang Li
Department of Chemistry, University of Western Ontario
London, Ontario, Canada, N6A 5B7
J. Anthony MacPhee
CANMET/ERL, 555 Booth Street
Ottawa, Ontario, Canada, K1A 0G1

Keywords: colorimetry, Fe^{3+} , coal

ABSTRACT

Solutions of $\text{FeCl}_3/\text{K}_3\text{Fe}(\text{CN})_6$ have been used to stain coal macerals. In this paper the development of a blue color in coal slurries in contact with $\text{Fe}^{3+}/\text{Fe}(\text{CN})_6^{3-}$ resulting from oxidation of the coal by Fe^{3+} is used as a measure of the reactivity of the coal surface.

INTRODUCTION

Salehi and Hamilton⁽¹⁾ have used iron salts to stain coal surfaces as an aid in optical and electron microscopy. The authors did not speculate on the chemistry involved in the staining process. We suggest that the development of blue colors on the coal surfaces following exposure to $\text{Fe}^{3+}/\text{Fe}(\text{CN})_6^{3-}$ solutions results from oxidation of the coal surface by Fe^{3+} with the subsequent formation of a charge-transfer complex (prussian blue) between $\text{Fe}^{2+}/\text{Fe}(\text{CN})_6^{3-}$. Since this complex absorbs strongly in the visible region the reaction can be followed by colorimetry of appropriate coal slurries. The kinetics of the Fe^{3+} reduction are a direct measure of the reactivity of individual coals and may provide a means of predicting coal quality in specific industrial useage.

EXPERIMENTAL

Five of the coals used were obtained from the Argonne Premium Coal Sample Program while an additional two coals, P851 and P832 were mid volatile bituminous coals from Western Canada, supplied by CANMET, Ottawa, Canada. All samples were 100 mesh.

Coal slurries were maintained at 30°C and stirred with a magnetic stir bar for periods ranging from five to twenty minutes. The slurries were then filtered to remove all solid matter. The resulting solutions were subjected to colorimetric analysis at 700 nm. Coal slurries were prepared in two different ways: a) 0.30 g of coal were added to a solution prepared by mixing 20 ml of 0.60 M FeCl_3 with 10 ml of 0.30 M K_3FeCN_6 - this method did not yield satisfactory results and was used only for one sample; b) 0.30 g of coal were added to 20 ml of 0.60 M FeCl_3 . This slurry was filtered after reaction with the coal and 10 ml of 0.30 M $\text{K}_3\text{Fe}(\text{CN})_6$, which served as an indicator of the Fe^{3+} /coal interaction, was added after filtration was complete.

RESULTS AND DISCUSSION

The coal P851 was used to test the two procedures used in preparing the coal slurries. Figure 1 shows the results obtained by procedure a) while Figure 2 shows the results from procedure b). The first procedure leads to little measurable reaction while the second yields a well defined increase in the concentration of Fe^{2+} with time. These results suggest that K^+ , $\text{Fe}(\text{CN})_6^{3-}$ and/or the $\text{Fe}^{2+}/\text{Fe}(\text{CN})_6^{3-}$ complex are strongly adsorbed on the coal surface and prevent further reaction of Fe^{3+} with the coal surface. The $\text{Fe}^{2+}/\text{Fe}(\text{CN})_6^{3-}$ seems to be the most likely explanation since Salehi and Hamilton observed a blue stain on coal surfaces after rinsing and drying coal surfaces identical to those used in preparing the coal slurries in procedure a). Accordingly procedure b) was used throughout the remainder of this study.

Figures 3-7 show the increase with Fe^{2+} concentration with time as well as the reaction rate obtained from the slope of this plot. In the case of the North Dakota coal only the first two points were used since the graph shows an initial fast reaction followed by a plateau with little further reaction. Figure 8 shows a plot of reaction rate vs O/C ratio for each of the Argonne coals.

It is clear that each coal yields a reaction rate which is strongly correlated with O/C ratio. The North Dakota coal shows an initial fast reaction while the other coals have an apparent non-zero intercept for Fe^{2+} in the Fe^{2+} vs time plot. This result may be due to an initial rapid reaction or to Fe^{2+} present in the coal prior to reaction.

CONCLUSIONS

Fe^{3+} , from FeCl_3 , in solution oxidizes coal surfaces and the resulting $\text{Fe}^{2+}/\text{Fe}^{3+}$ charge transfer complex may be used as an indicator of the extent of reaction when Fe^{3+} is introduced as $\text{Fe}(\text{CN})_6^{3-}$.

The $\text{Fe}^{2+}/\text{Fe}(\text{CN})_6^{3-}$ is strongly adsorbed on the coal surface and inhibits further reaction. The kinetics of the Fe^{3+} reduction can be followed colorimetrically if $\text{K}_3\text{Fe}(\text{CN})_6$ is added to solutions obtained from coal slurries in contact with FeCl_3 .

The kinetics of Fe^{3+} reduction can be correlated with the O/C ratio in the coal.

REFERENCE

1. MORTAZA R. SALEHI and LLOYD H. HAMILTON. Surface-reaction of Australian coal macerals and coke by iron salts: an aid in microscopy. *Fuel*, 1988, 67, 296-297.

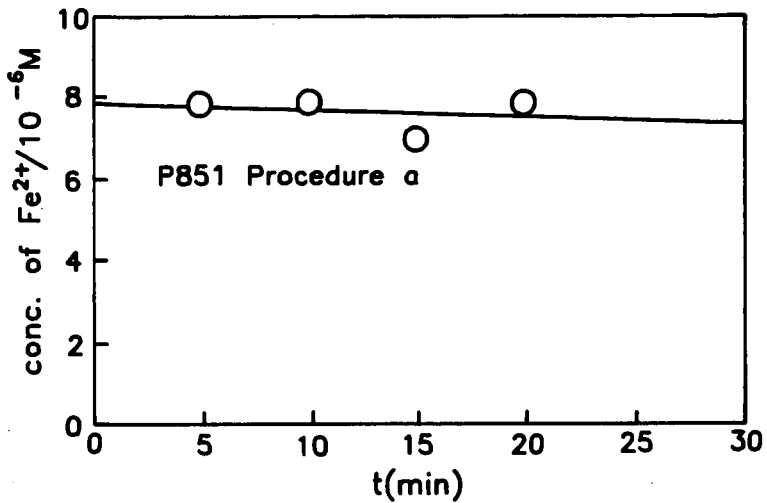


Figure 1

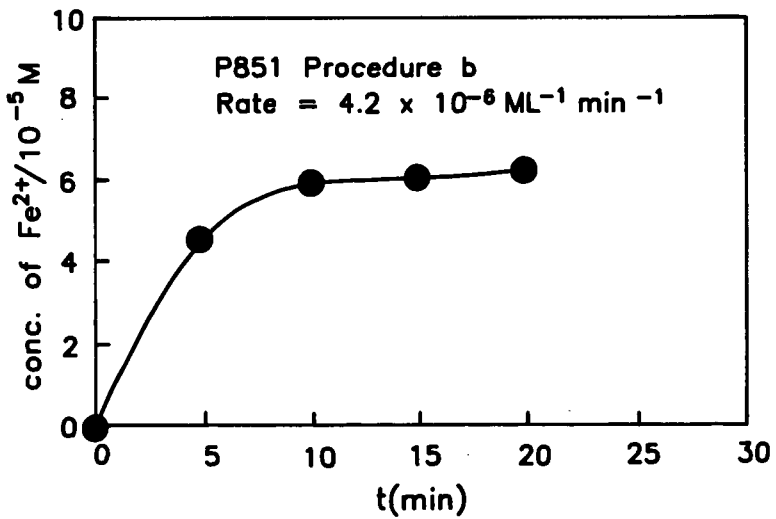


Figure 2

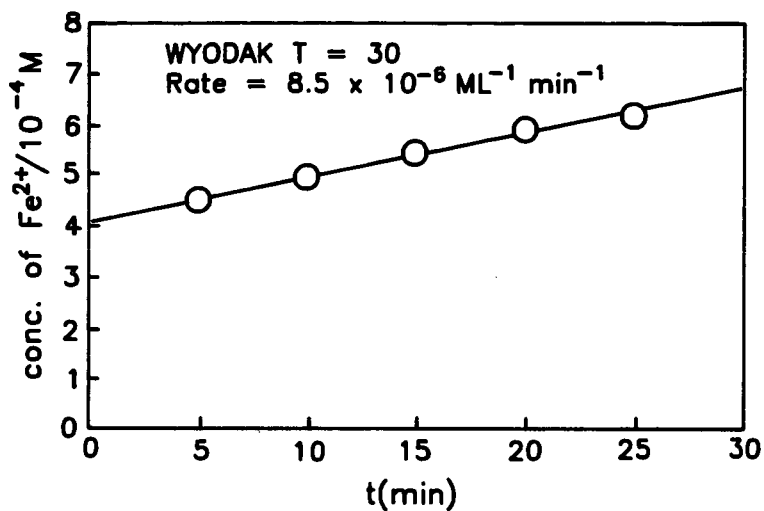


Figure 3

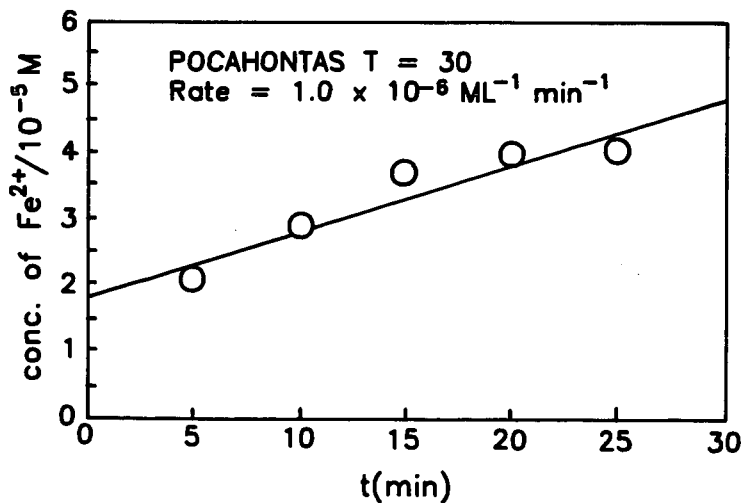


Figure 4

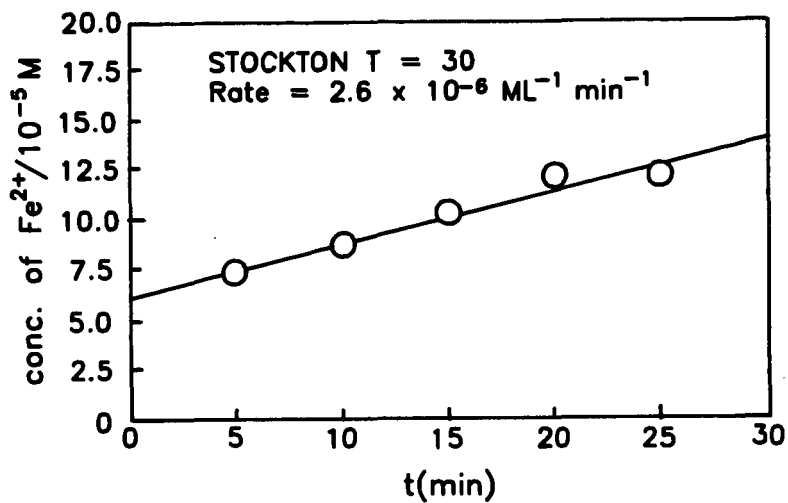


Figure 5

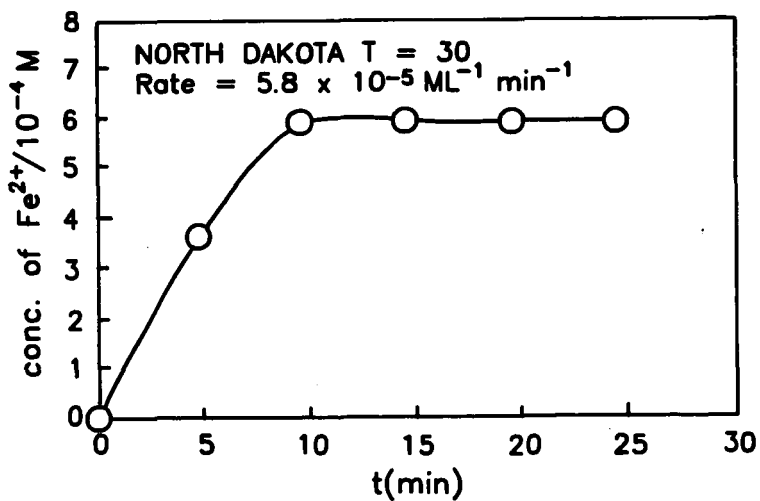


Figure 6

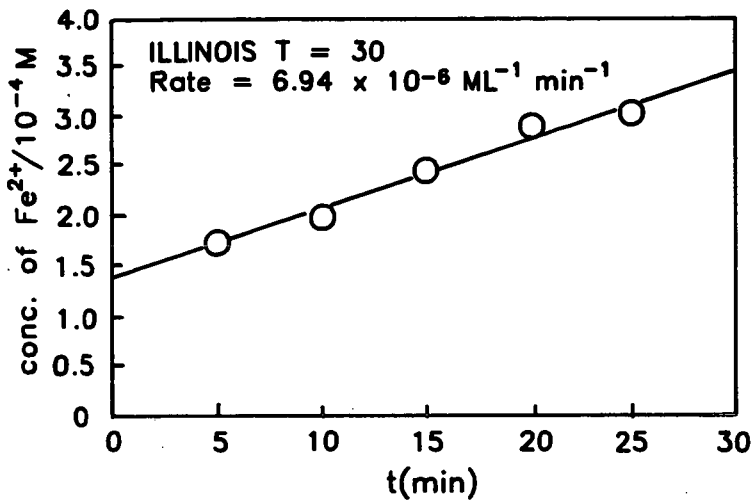


Figure 7

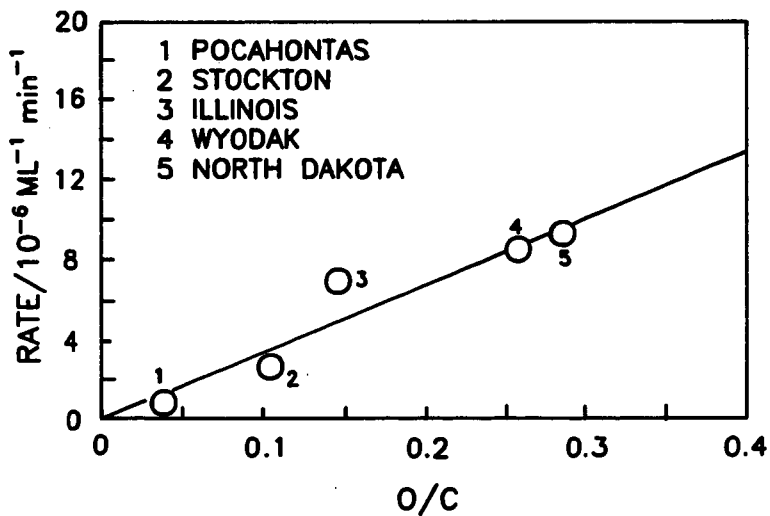


Figure 8